TECHNICAL REPORT

ISO/TR 5602

First edition
2021-11

Sources of error in the use of electrochemical impedance spectroscopy for the investigation of coatings and other materials

Sources d'erreur dans l'utilisation de la spectroscopie d'impédance électrochimique pour l'étude des revêtements et autres matériaux

Reference number
ISO/TR 5602:2021(E)

ISO copyright office
CP 401 • Ch. de Blandonnet 8
CH-1214 Vernier, Geneva
Phone: +41 22 749 01 11
Email: copyright@iso.org
Website: www.iso.org

Published in Switzerland

Contents

Page

Foreword

ISO (the International Organization for Standardization) is a worldwide federation of national standards bodies (ISO member bodies). The work of preparing International Standards is normally carried out through ISO technical committees. Each member body interested in a subject for which a technical committee has been established has the right to be represented on that committee. International organizations, governmental and non-governmental, in liaison with ISO, also take part in the work. ISO collaborates closely with the International Electrotechnical Commission (IEC) on all matters of electrotechnical standardization.

The procedures used to develop this document and those intended for its further maintenance are described in the ISO/IEC Directives, Part 1. In particular, the different approval criteria needed for the different types of ISO documents should be noted. This document was drafted in accordance with the editorial rules of the ISO/IEC Directives, Part 2 (see www.iso.org/directives).

Attention is drawn to the possibility that some of the elements of this document may be the subject of patent rights. ISO shall not be held responsible for identifying any or all such patent rights. Details of any patent rights identified during the development of the document will be in the Introduction and/or on the ISO list of patent declarations received (see www.iso.org/patents).

Any trade name used in this document is information given for the convenience of users and does not constitute an endorsement.

For an explanation of the voluntary nature of standards, the meaning of ISO specific terms and expressions related to conformity assessment, as well as information about ISO's adherence to the World Trade Organization (WTO) principles in the Technical Barriers to Trade (TBT), see www.iso.org/iso/foreword.html.

This document was prepared by Technical Committee ISO/TC 35, *Paints and varnishes*, Subcommittee SC 9, *General test methods for paints and varnishes*.

Any feedback or questions on this document should be directed to the user's national standards body. A complete listing of these bodies can be found at www.iso.org/members.html.

Introduction

Electrochemical impedance spectroscopy is described in detail in ISO 16773-1 to ISO 16773-4. It became apparent during use of these standards that sources of error and measurement artefacts that lead to incorrect interpretations are not dealt with comprehensively. This document supplements the ISO 16773 series of standards to deal with this issue.

Sources of error in the use of electrochemical impedance spectroscopy for the investigation of coatings and other materials

1 Scope

This document describes the main sources of error in the use of electrochemical impedance spectroscopy for the investigation of coatings and other materials. The sources of error listed here include all process steps from the set-up of the sample with the measuring cell right through to evaluation.

NOTE The sources of error discussed here do not represent a complete list.

2 Normative references

The following documents are referred to in the text in such a way that some or all of their content constitutes requirements of this document. For dated references, only the edition cited applies. For undated references, the latest edition of the referenced document (including any amendments) applies.

ISO 4618, *Paints and varnishes — Terms and definitions*

ISO 16773-1, *Electrochemical impedance spectroscopy (EIS) on coated and uncoated metallic specimens — Part 1: Terms and definitions*

3 Terms and definitions

For the purposes of this document, the terms and definitions given in ISO 4618, ISO 16773-1 and the following apply.

ISO and IEC maintain terminology databases for use in standardization at the following addresses:

— ISO Online browsing platform: available at https://www.iso.org/obp

— IEC Electropedia: available at https://www.electropedia.org/

3.1
limit impedance
minimum or maximum impedance that can be measured using the impedance spectrometer

3.2
limit frequency
minimum or maximum frequency that can be set on the impedance spectrometer

4 Error in the make-up of the measuring cell

4.1 Roughness of the surface

A wet and rough surface could conduct stray currents to a scratch or artificial defect, see Figure 1. This could yield in a spectrum showing a much lower resistance than in reality. Examples of spectra are shown in Figure 2.

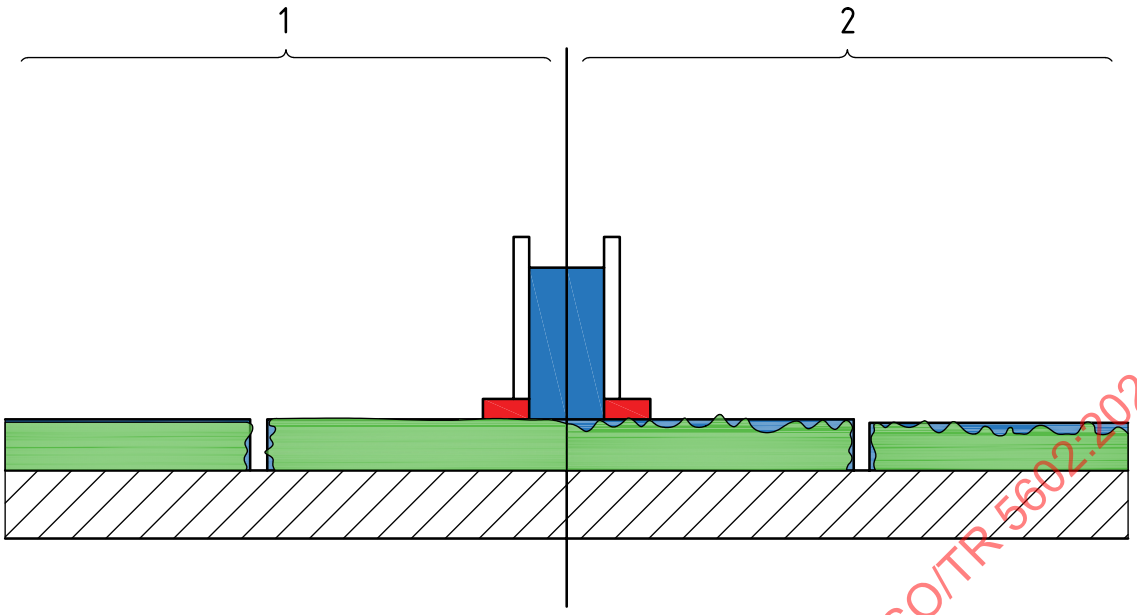

Key

1 without UV-irradiation
2 after UV-irradiation
PMMA tube
seal
coating
electrolyte
steel

Figure 1 — Conductive path from counter electrode to scratch due to surface roughness

The rough surface was measured on the unscratched area. Although the rough surface was dried with a tissue, the residual amount of water was sufficient to produce a conductive path via the scratch to the substrate. As result, the spectrum of the sample resulted in the incorrect identification of a defective coating. After 2 h of continuous immersion in the cell, the surface outside the cell had dried and the conductive path was interrupted, which resulted in a typical spectrum of an intact coating.

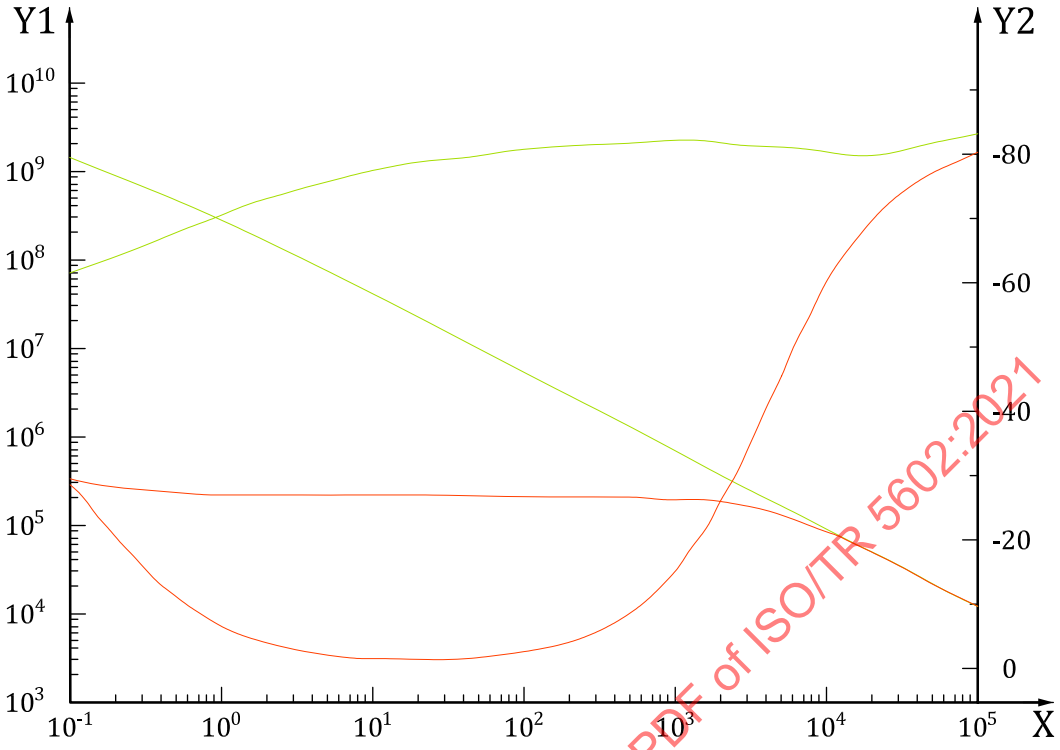

Key

X	frequency, f, in Hz
Y1	impedance, Z, in Ω
Y2	phase angle, φ, in degrees
	2 h drying
	wet

Figure 2 — EIS spectra of the initially wet coating and 2 h after drying

4.2 O-ring — Considerations about the precise determination of the exposed area

If an O-ring is used to seal the cell, the exposed area is smaller than the theoretically assumed area because the O-ring will be compressed, and therefore, the exposed area will be reduced (see Figure 3).

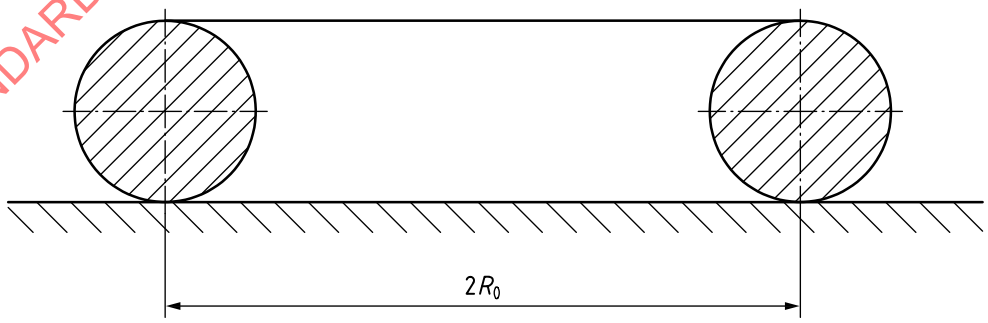

a) Ideal situation, uncompressed

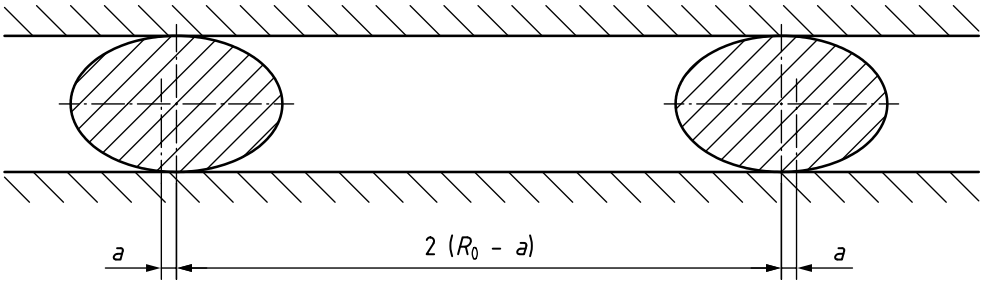

b) Real situation, compressed

Key

R_0 radius of the uncompressed O-ring

a difference in the radius of the O-ring due to compression

Figure 3 — Uncompressed and compressed O-ring

This behaviour can be visualized easily by using two transparent PMMA (poly-methylene methacrylate) plates which were compressed with 4 screws. The screws were gently tightened only by hand and without any tools.

Figure 4 shows the set-up and Figure 5 and Figure 6 show the compressed O-rings of 1,2 cm and 5 cm diameter, respectively.

Figure 4 — Compression of O-ring using 4 screws

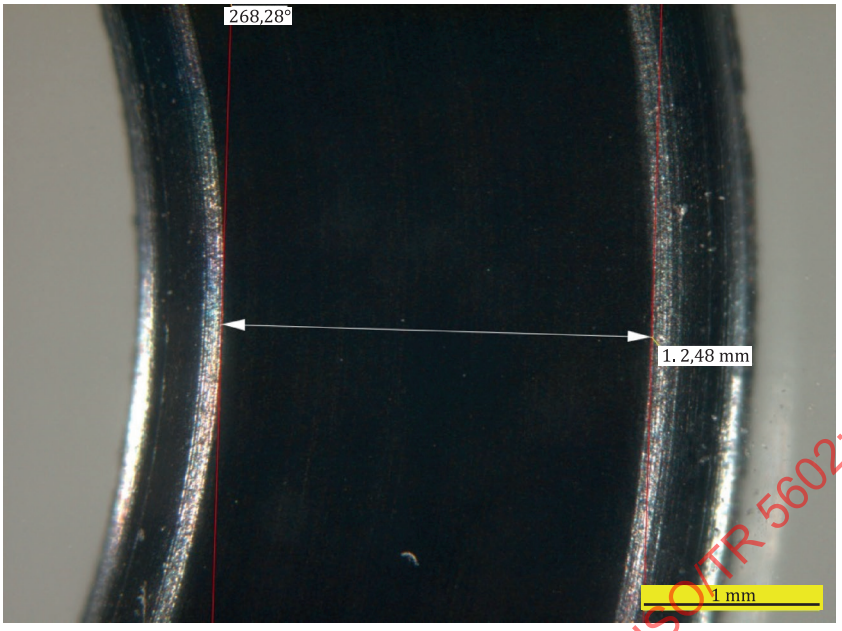

Figure 5 — Compressed O-ring of 1,2 cm diameter

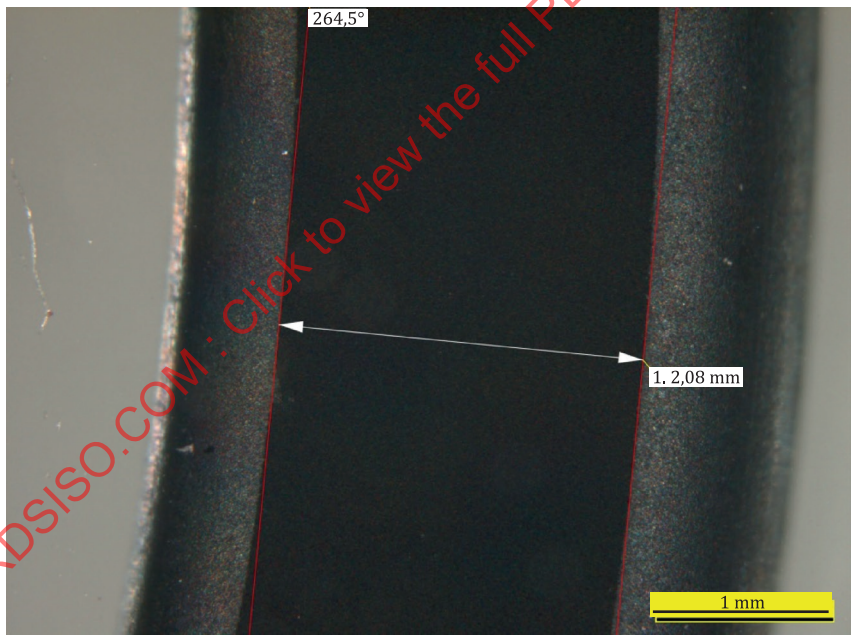

Figure 6 — Compressed O-ring of 5 cm diameter

The exposed area can be calculated as illustrated in Figure 7.

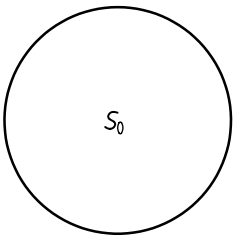

$$S_0 = \pi \cdot R_0^2$$

a) O-ring not compressed — Contact surface of the specimen with testing solution

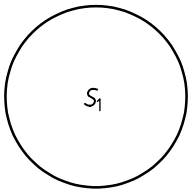

$$S_1 = \pi \cdot (R_0 - a)^2$$

b) O-ring compressed — Contact surface of the specimen with testing solution

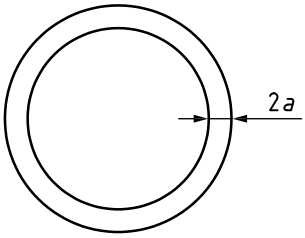

$$\Delta S = S_0 - S_1 = \pi \cdot R_0^2 - \pi \cdot (R_0 - a)^2$$

c) Reduction of contact surface of specimen due to O-ring compression

Key

S_0 geometric area with the O-ring uncompressed
S_1 exposed area with the O-ring compressed
ΔS difference $S_0 - S_1$
R_0 radius of the uncompressed O-ring
a difference of the radius of the O-ring due to compression

Figure 7 — Calculation of the exposed area

The error dS between exposed area S_1 and geometric area S_0 can be approximated depending on the O-ring radius, R_0, and the measured contact, $2a$, using Formula (1):

$$dS = \frac{\Delta S}{S_0} \cdot 100 = \frac{2 \cdot a \cdot R_0 \cdot a^2}{R_0^2} \cdot 100 \quad (1)$$

Some examples for calculation of the error of the exposed area are shown in Table 1.

Table 1 — Approximate error estimation of contact surface of specimens in corrosion cells

Radius of the uncompressed O-ring	Difference in the radius of the O-ring due to compression		Geometric area with the O-ring uncompressed (theoretical surface)	Exposed area with the O-ring compressed (real surface)	Error of the exposed area
R_0 mm	a mm	$R_0 - a$ mm	S_0 mm^2	S_1 mm^2	dS %
6	0,8	5,2	113	85	25
12	0,8	11,2	452	394	13
24	0,8	23,2	1 809	1 690	7
30	0,8	29,2	2 826	2 677	5
6	1	5	113	79	31
12	1	11	452	380	16
24	1	23	1 809	1 661	8
30	1	29	2 826	2 641	7
6	1,25	4,75	113	71	37
12	1,25	10,75	452	363	20
24	1,25	22,75	1 809	1 625	10
30	1,25	28,75	2 826	2 595	8

4.3 Faulty cell make-up

4.3.1 Optically detectable leaks

Optically detectable leaks in the measuring cell are obvious and are not dealt with here.

4.3.2 Optically non-detectable causes

The behaviour shown in Figure 8 was observed in a non-reproducible manner for a very well-documented coating (cathodic e-coat) that is in familiar use in measurement technology. This behaviour occurred with varying amounts of pressure on the measuring cell at different locations on the same test panels; however, a direct relationship was not detected.

If the behaviour shown in Figure 8 is observed in a measuring cell, the measuring cell is not suitable.

Generally, every measurement set-up is tested for errors with a familiar system before this measuring cell is used on an unfamiliar system.

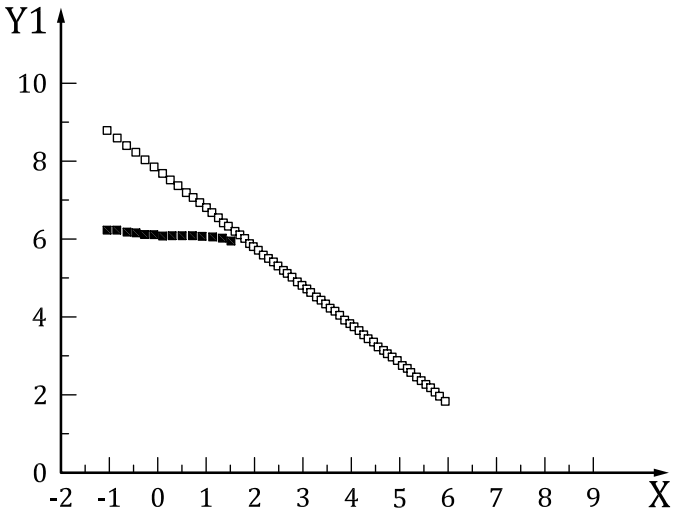

a) Magnitude of impedance as a function of frequency

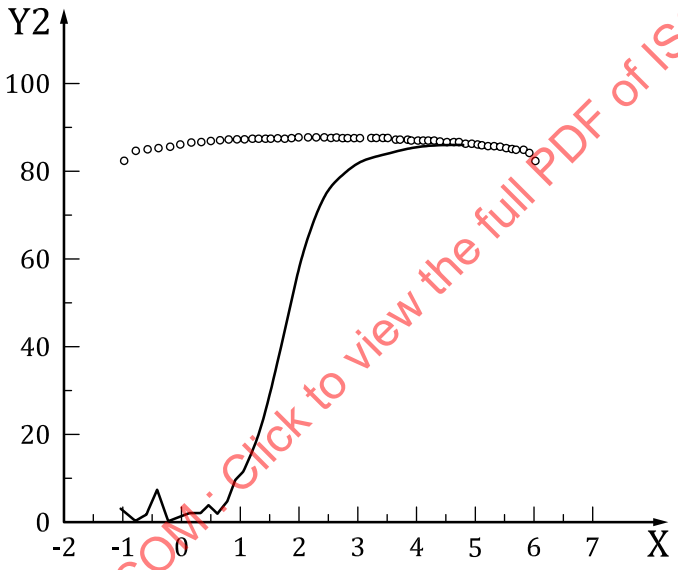

b) Phase angle as a function of frequency

Key

X	logarithm of the frequency, log f, in Hz
Y1	logarithm of the modulus of the impedance, log $\|Z\|$, in $\Omega \cdot cm^2$
Y2	absolute value of the phase angle, φ, in degrees
■	wrong sealing
□	sealing correct
———	wrong sealing
○	sealing correct

Figure 8 — Possible influence of a faulty cell set-up

4.4 Reference electrodes

4.4.1 General information on the distance between the reference and working electrodes

RE1, RE2 and RE3 as shown in Figure 9 are the various positions where the reference electrode RE can be placed to measure the potential. At distances very close to the working electrode, the equipotential lines are close together and small variations in the position of the reference electrode can lead to large variations in the ohmic drop. This applies in particular to uncoated samples. In some cases, it is preferable not to use a Luggin capillary, and instead to place the reference electrode far from the working electrode and measure and compensate for the ohmic drop.

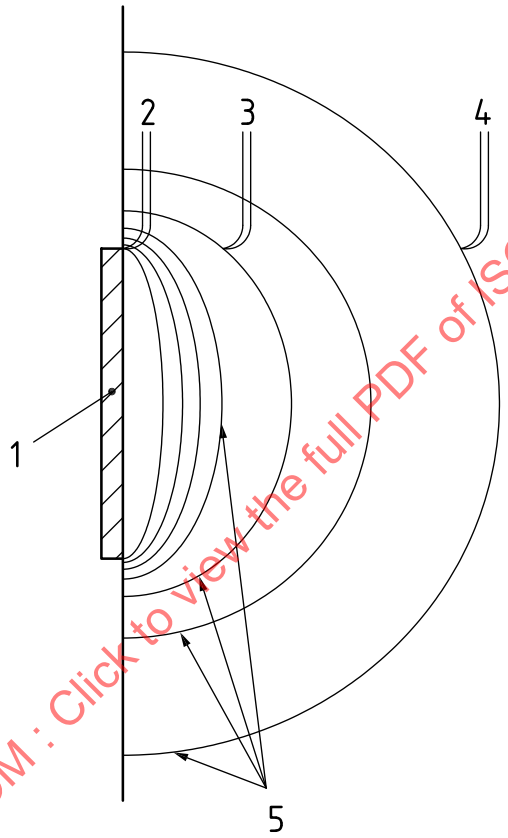

Key

1 working electrode (WE)
2 reference electrode 1 (RE 1)
3 reference electrode 2 (RE 2)
4 reference electrode 3 (RE 3)
5 equipotential lines

Figure 9 — Equipotential lines shown at close proximity to the working electrode

The influence of the reference electrode distance is negligible for measurements on coated (high-resistance) samples. See Figure 10.

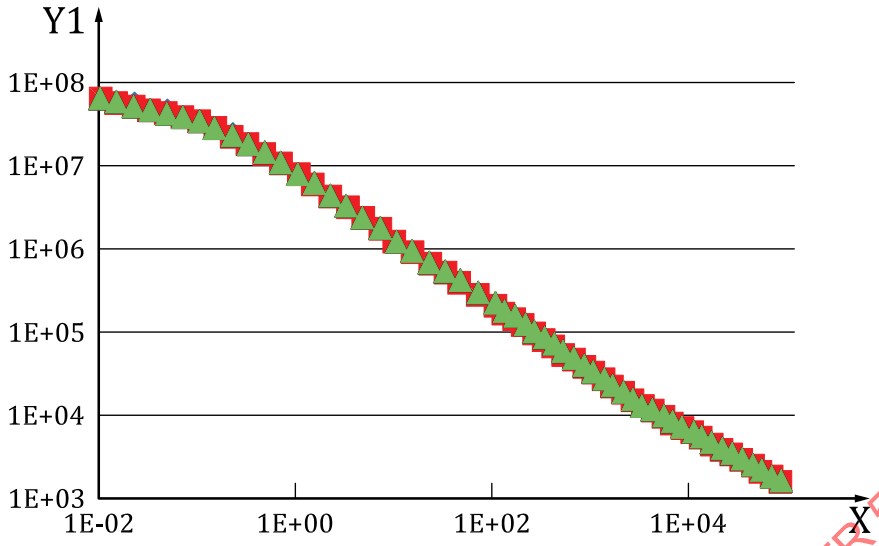

a) Three |*Z*| curves are shown here that were recorded with different distances between the reference electrode and working electrode. The distances to the coated substrate are 37 mm (top), 15 mm (middle) and 2 mm (bottom).

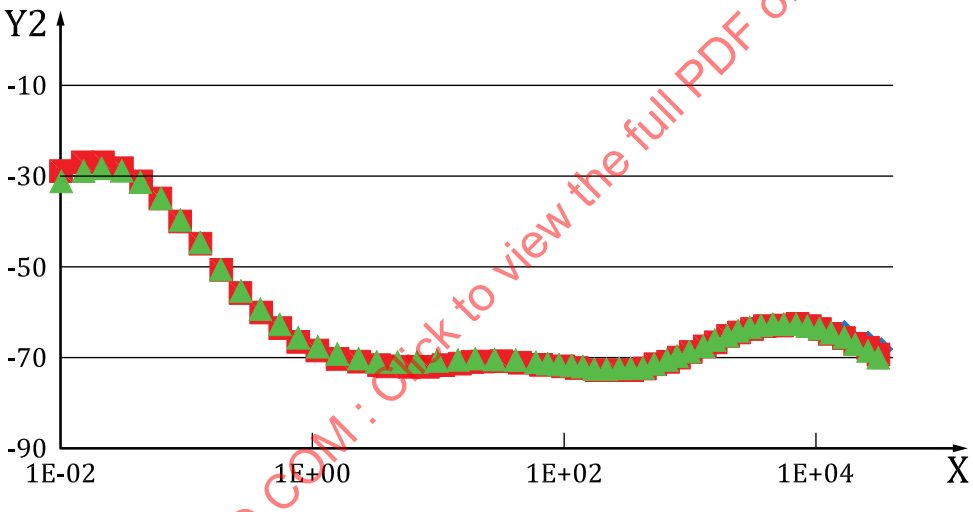

b) Three phase angle curves are shown here that were recorded with different distances between the reference electrode and working electrode. The distances to the coated substrate are 37 mm (top), 15 mm (middle) and 2 mm (bottom).

Key

X1 frequency, *f*, in Hz
X2 frequency, *f*, in Hz
Y1 modulus of the impedance, |*Z*|, in $\Omega \cdot cm^2$
Y2 absolute value of the phase angle, φ, degrees
◆ top (mostly invisible due to overlayings with the middle and bottom data points)
■ middle
▲ bottom

Figure 10 — Spectra of coated (high-resistance) samples

4.4.2 Shielding

If the distance between the reference electrode and working electrode is too small, the electrical field is shielded, and this leads to an undefined state. Shielding of the working electrode by the reference electrode can only occur as a problem with the Haber-Luggin capillary, as there is a very small distance between the capillary opening and working electrode in this case.

4.4.3 Air bubble in the reference electrode

An air bubble in the reference electrode leads to undefined potentials and can result in strong oscillations in the phase.

4.4.4 Poisoning of the reference electrode

Poisoning of the reference electrode occurs when ions or molecules diffuse into the electrode and react with the reference material. This results in a potential shift. This effect is less significant with a coated electrode than with a metallic electrode.

Poisoning of the reference electrode can largely be prevented by hydrostatic effects and by correctly positioning the electrode.

The use of a Haber-Luggin electrode can be effective in order to delay poisoning of the reference electrode.

4.4.5 Bleeding of the reference electrode

Diffusion of ions from the reference electrode into the electrolyte is referred to as bleeding of the reference electrode. These ions can alter the reaction at the working electrode.

The use of a Haber-Luggin electrode can be effective in order to delay bleeding of the reference electrode.

4.5 Counter electrodes

4.5.1 Relative sizes

For coated samples, there are no known artefacts that can be ascribed to an unsuitable choice of relative sizes of the working electrode and counter electrode. This can be explained by the very low currents in the measurement of these high-resistance systems. However, the area of the counter electrode is chosen as large as possible.

4.5.2 Reactive counter electrodes

As regards the make-up of measuring cells, the counter electrode consists of a material that is inert to the electrolyte over the period of measurement. If there are doubts as to the suitability of the counter electrode material, comparative measurements are carried out on different materials with a known reference sample. Exposure experiments are also carried out.

4.6 Gas inclusions in the measuring cell

Despite the influence of gas bubbles in the measuring cell that is to be expected theoretically, this could not be verified in a test experiment with gas bubbles on the counter electrode, see Figure 11. A single-layer test coating was measured.

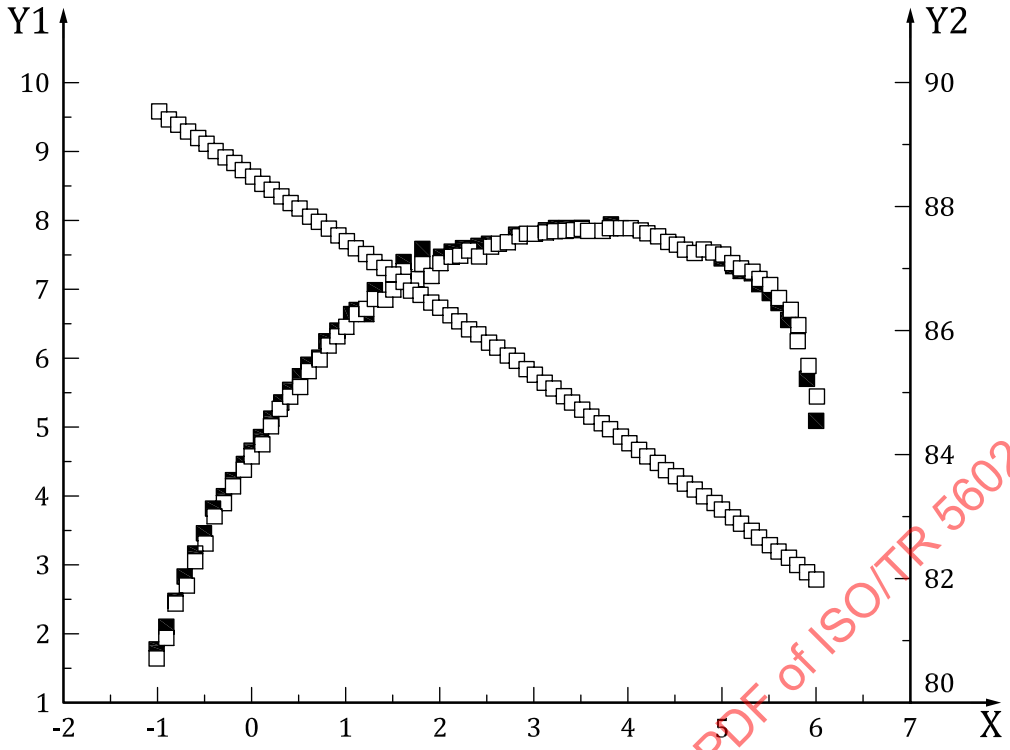

Key

X logarithm of the frequency, log f, in Hz

Y1 logarithm of the modulus of the impedance, log $|Z|$, in $\Omega \cdot cm^2$

Y2 absolute value of the phase angle, φ, in degrees

■ with air bubbles

□ without air bubbles

Figure 11 — Bode plots for two measurements with and without gas bubbles on the counter electrode

The reduction of the effective area caused by gas-bubble absorption at the working electrode has an influence on the measurement values of the layer capacitance and layer resistance.

5 Faults caused by electronics incl. shielding

5.1 Faraday cage

Any discontinuities in the phase angle plot at 50 Hz are probably due to insufficient shielding. See Figure 12.

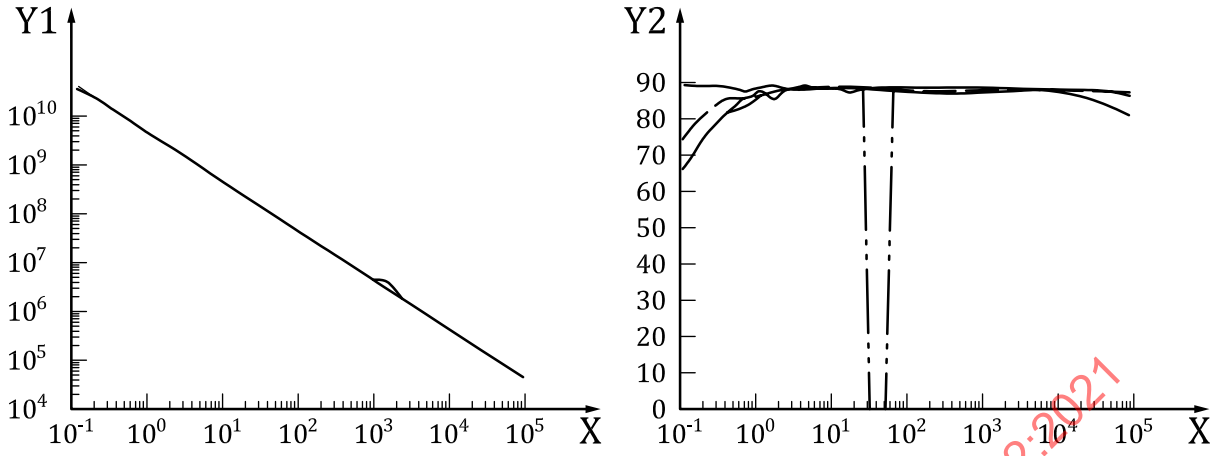

Key

X	frequency, f, in Hz
Y1	modulus of the impedance, $\|Z\|$, in $\Omega \cdot cm^2$
Y2	absolute value of the phase angle, φ, in degrees
————	t = 0 h
— — —	t = 10 h
- - - - - - - -	t = 20 h
— · —	t = 40 h
— - - —	t = 70 h

Figure 12 — Dramatic grid frequency influence visible on a Bode plot

Figure 12 shows a dramatic example for grid frequency influences, whereas Figure 13 shows negligible disturbance.

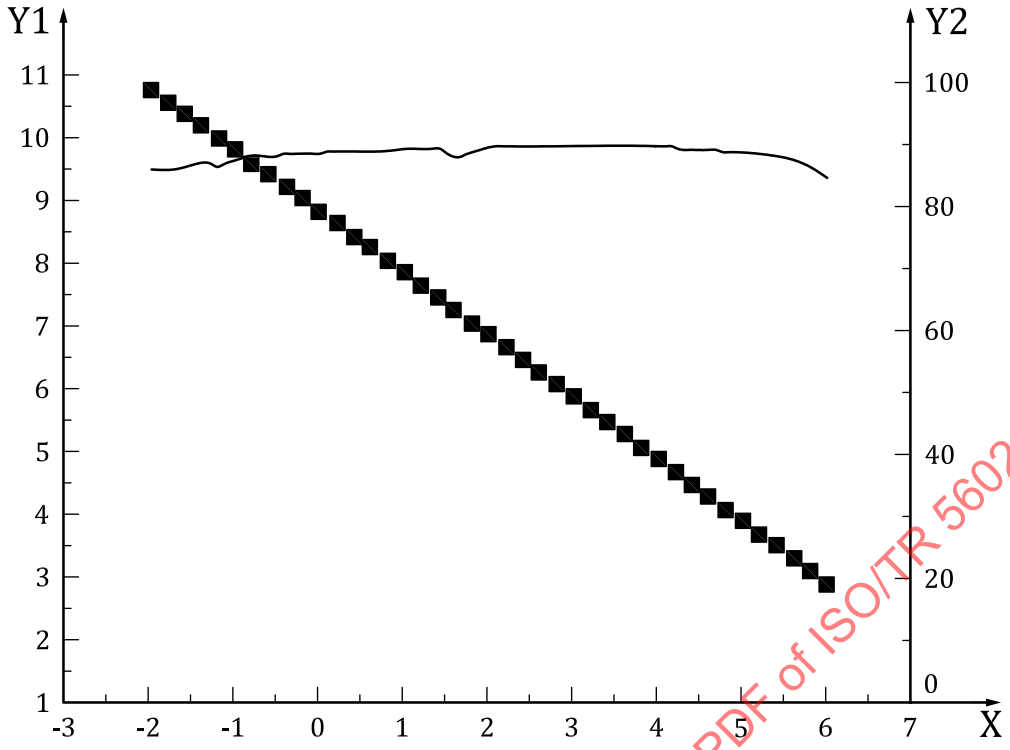

Key

X	logarithm of the frequency, log f, in Hz
Y1	logarithm of the modulus of the impedance, log $\|Z\|$, in $\Omega \cdot cm^2$
Y2	absolute value of the phase angle, φ, in degrees
———	phase angle
■	impedance

Figure 13 — Negligible grid frequency influence visible on a Bode plot

Figure 14 shows a magnified representation of the phase plot; the phase plot reacts particularly sensitively to grid frequency influences.

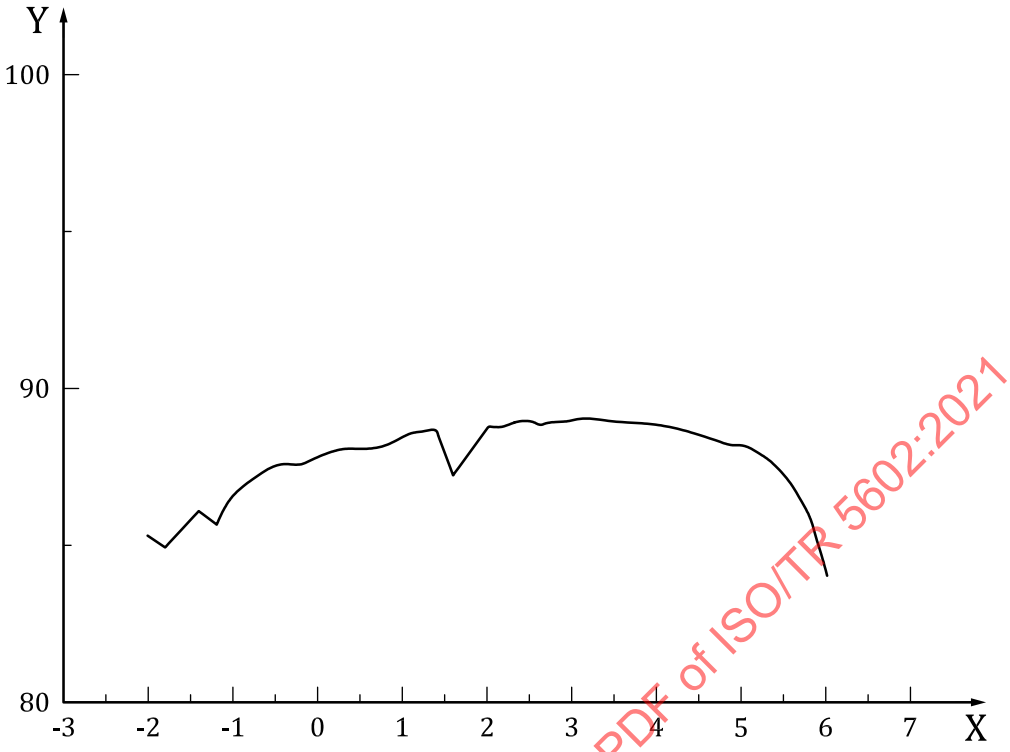

Key

X logarithm of the frequency, log *f*, in Hz

Y absolute value of the phase angle, φ, in degrees

Figure 14 — Magnified representation of the phase plot

5.2 Extended cable (without active shielding)

Figure 15 shows the phase plot of a measurement of a 330-pF capacitor. The yellow dots show the result with shielded cables; the cables were extended without active shielding in the case of the red and green curves, and the cables were also twisted in the case of the green curve. The amplitude was 10 mV. It is observed that significantly more interference signals are received in the case of the extension with unshielded cables.

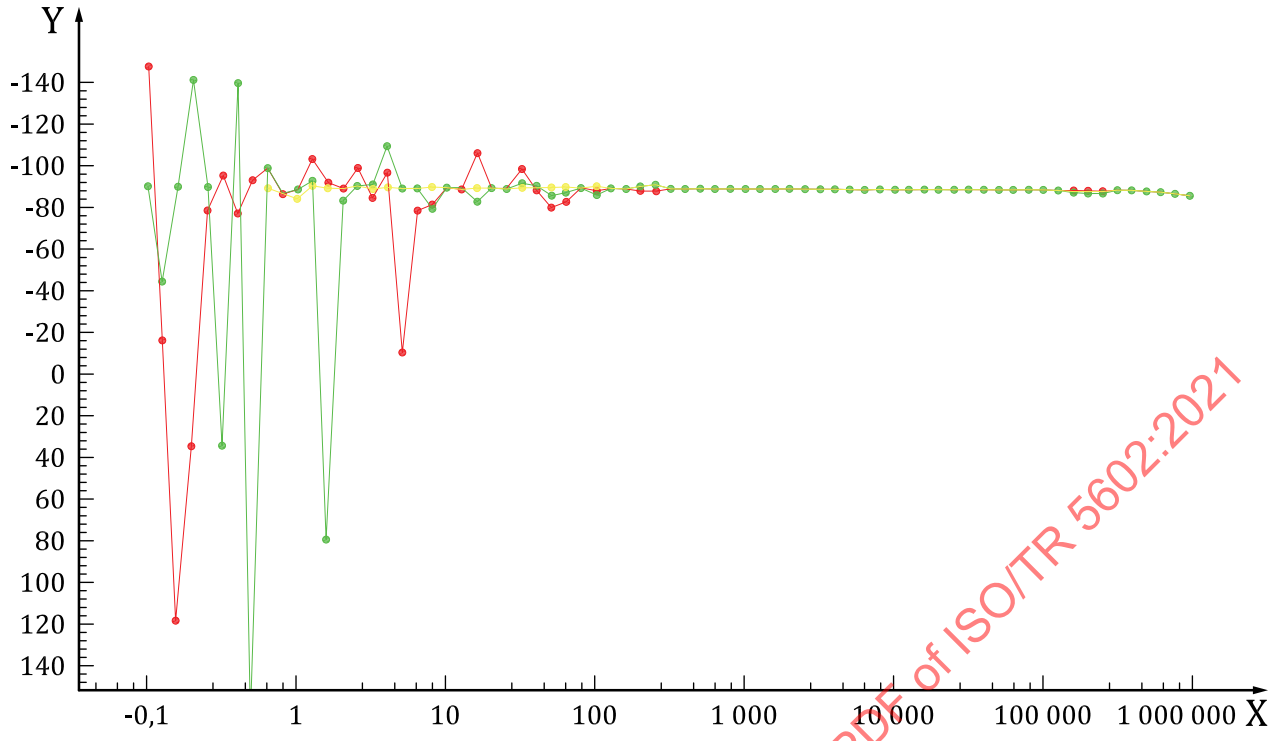

Key

X frequency, f, in Hz

Y phase angle, φ, in degrees

result with shielded cables

result with unshielded cables

result with unshielded cables and twisted in comparison to the red curve

Figure 15 — Phase plot of a measurement of a 330-pF capacitor

5.3 Cable breaks

In Figure 16, deviations from the real state can be seen that are caused by a cable break. The same dummy cell was measured in each case. After the measurement with the broken cable, the measurement was repeated with a new cable.

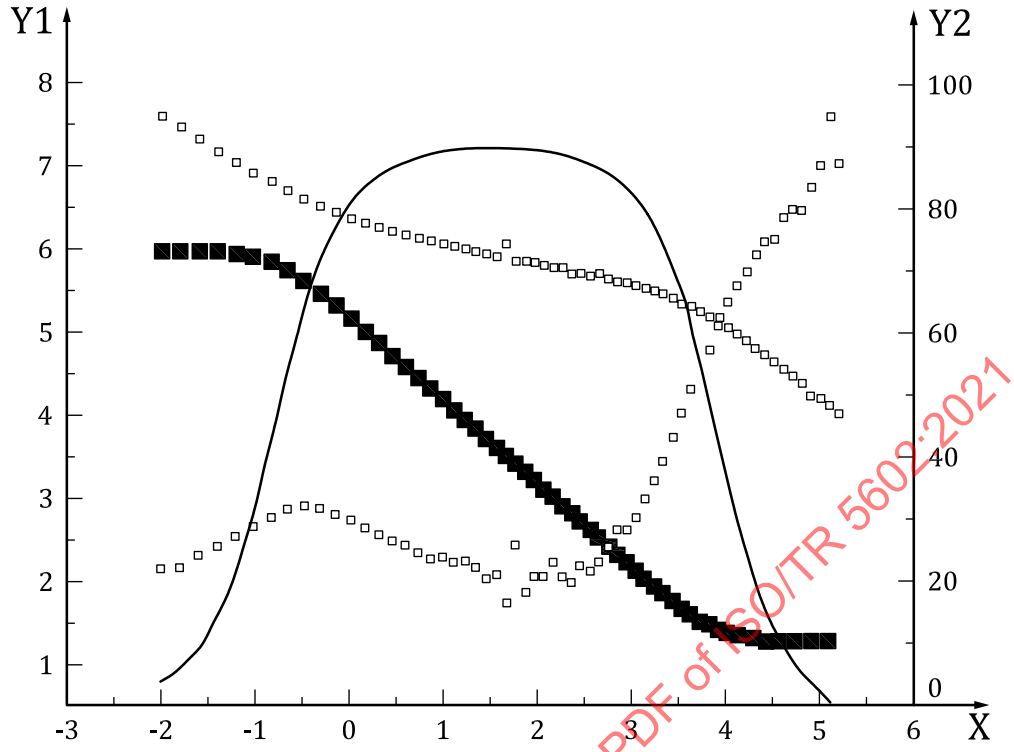

Key

X logarithm of the frequency, log f, in Hz

Y1 logarithm of the modulus of the impedance, log $|Z|$, in Ω

Y2 absolute value of the phase angle, φ, in degrees

▫ failure cable

■ efficient cable

Figure 16 — Measurement of a dummy cell with and without cable break

5.4 Contact resistances between metallic contacts and the working electrode/counter electrode

The profile shown in Figure 17 can occur if corroded connections are used (e.g. alligator clamps).

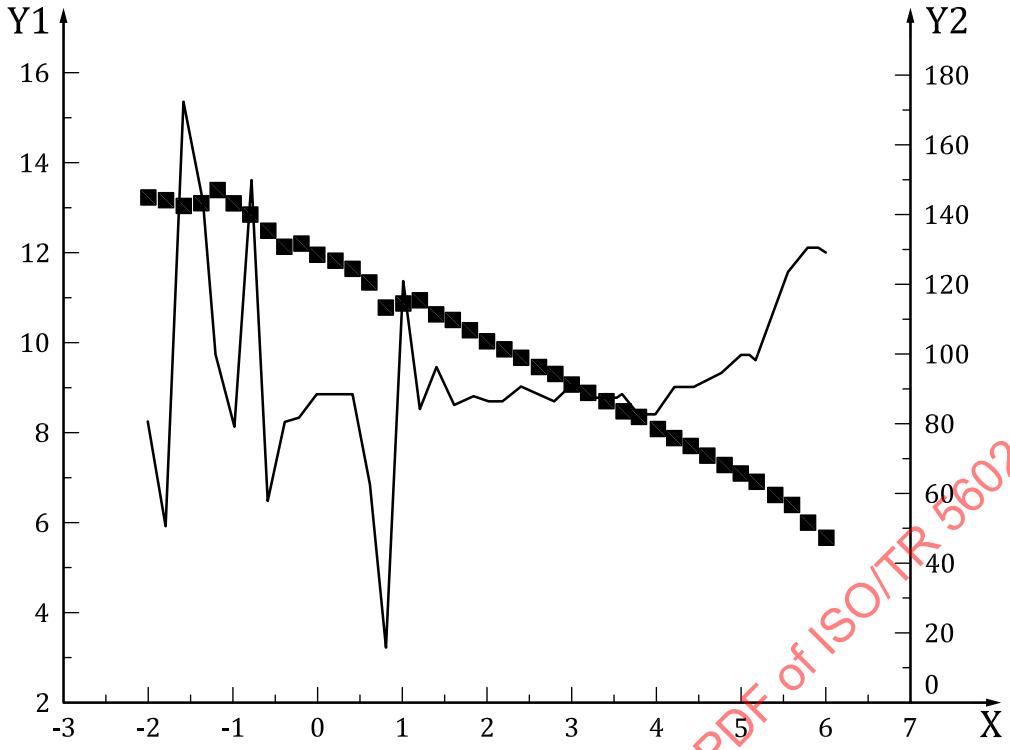

Key

X	logarithm of the frequency, log f, in Hz
Y1	logarithm of the modulus of the impedance, $\|Z\|$, in in $\Omega \cdot cm^2$
Y2	absolute value of the phase angle, φ, in degrees
■	impedance
———	phase angle

Figure 17 — Measurement with corroded connections

5.5 Inductivities

Inductivities can be caused by connection cables that are too long/twisted in the high-frequency range above 10 000 Hz. This influence is shown in Figure 18. The inductivity can be observed from the change in the sign of the phase. Because absolute values of the phase angle are plotted in the diagram, the curve of the phase angle is reflected instead of crossing the x-axis at Y2 = 0.

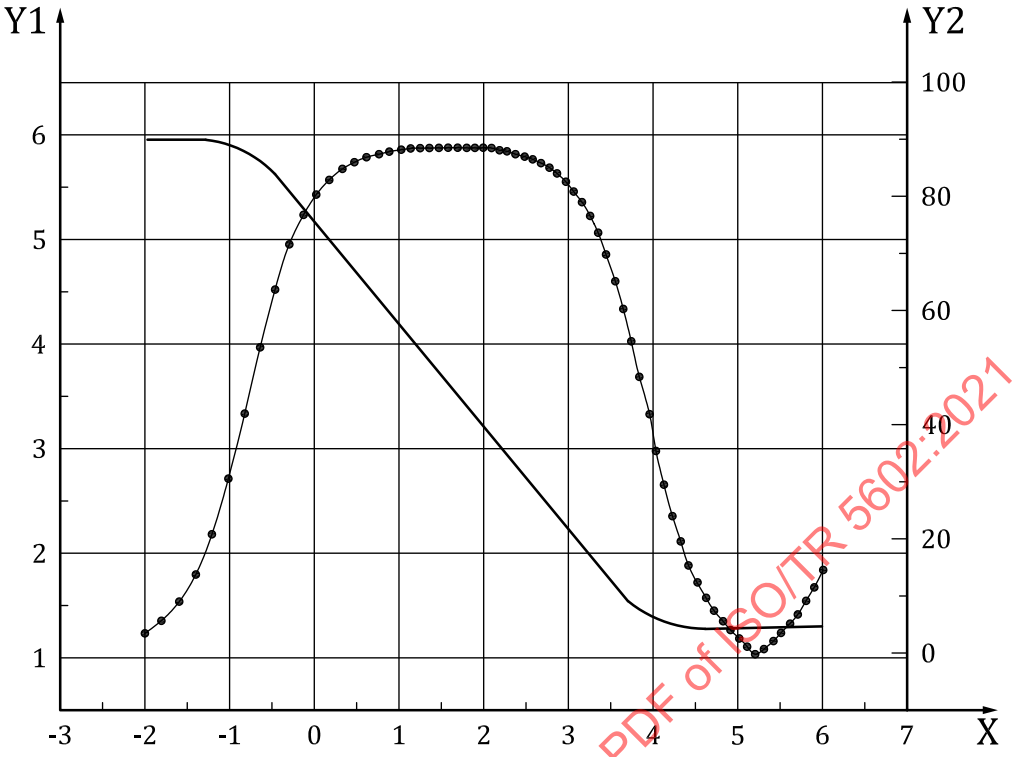

Key

X	logarithm of the frequency, log f, in Hz
Y1	logarithm of the modulus of impedance, log $\|Z\|$, in Ω
Y2	absolute value of the phase angle, φ, in degrees
•	phase angle
———	impedance

Figure 18 — Measurement with a cable that is too long between the measurement set-up and measuring device

5.6 Measurement range switching

Commercially available impedance spectrometers require several current measurement ranges over the entire frequency range. These current measurement ranges are automatically adapted by switching during the measurement. If switching between measurement ranges is not perfectly coordinated or if the calibration data are corrupt, a discontinuity in the phase plot can be observed. This is shown in Figure 19 b). This phenomenon occurs almost exclusively in the case of very high-resistance, low-capacitance systems.

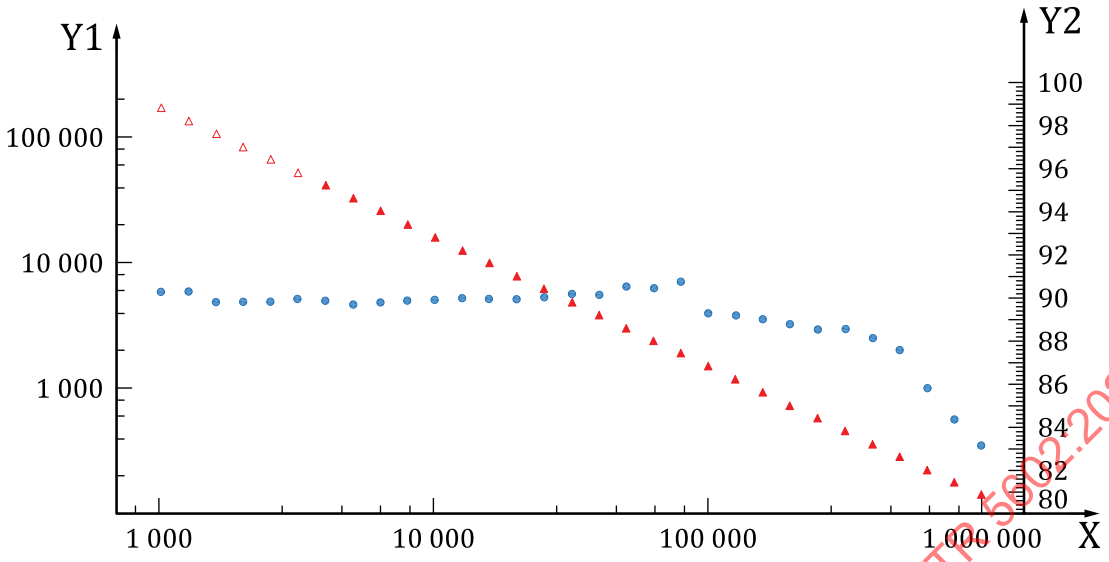

a) Despite calibration, measurement range switching can be detected by the jump in the phase plot.

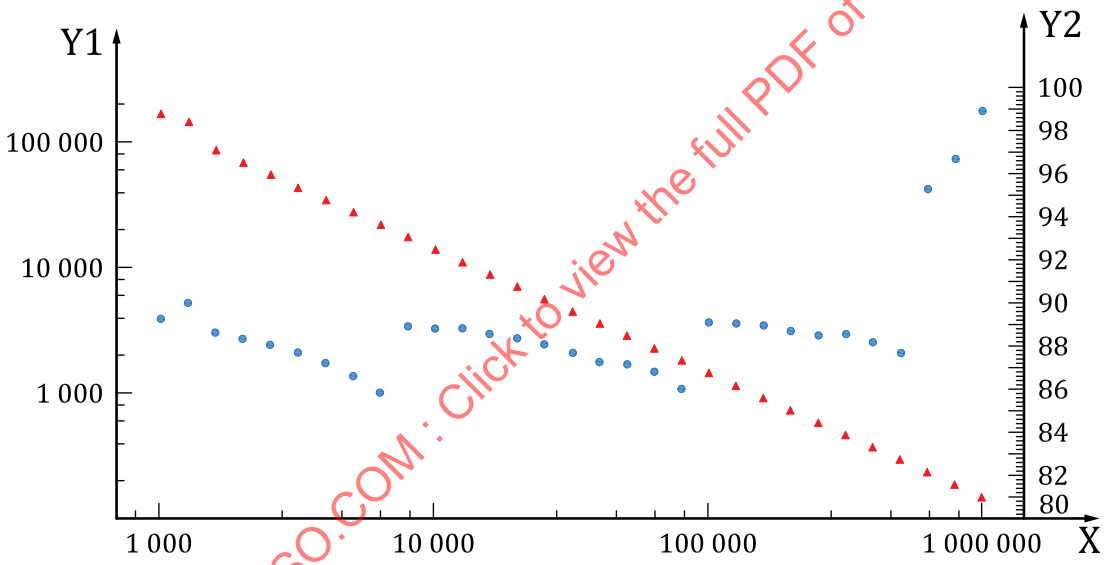

b) In the case of a non-calibrated system, the measurement range switching is clearly detectable in the phase plot.

Key

X frequency, f, in Hz
Y1 impedance, Z, in Ω
Y2 absolute value of the phase angle, φ, in degrees
▲ impedance
● phase angle

Figure 19 — Characteristics of measurement range switching for high-resistance, low-capacitance systems (a section of the entire spectrum is shown)

5.7 Scattering signals in power supply

The quality of measurement depends on the quality of the power supply. If the grid frequency has other frequencies, e.g. from generators or electromotive drives, superimposed on it, this can lead to impure

frequency signals in impedance spectroscopy. This can be rendered visible by carrying out a Fourier transform of the measurement signal. See Figure 20 b).

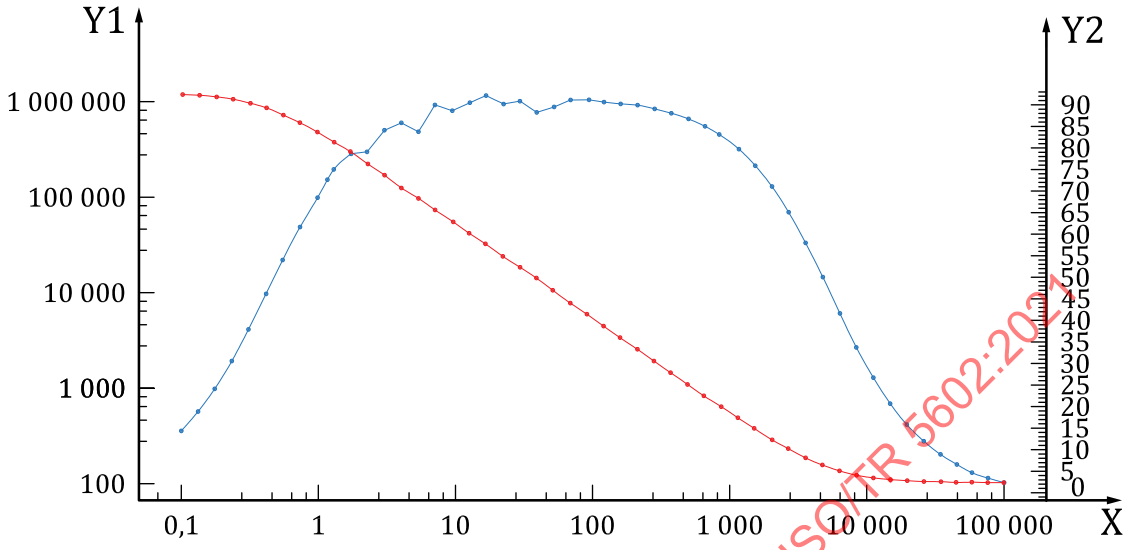

a) Example of impedance spectra with scattered data due to the influence of the power supply

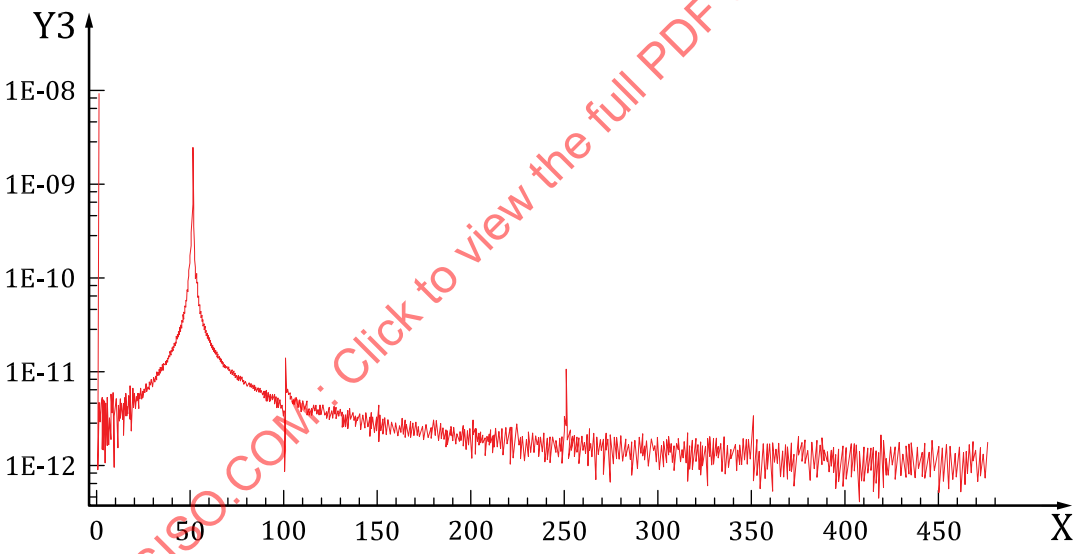

b) Fourier transform: harmonics of the 50 Hz disturbance are clearly detectable at 100 Hz, 250 Hz and 350 Hz

Key

X frequency, f, in Hz
Y1 impedance, Z, in Ω
Y2 absolute value of the phase angle, φ, in degrees
Y3 current, I, in A
impedance
phase angle
current

Figure 20 — Effects of a disturbance frequency (50 Hz)

5.8 Insufficient signal-to-noise ratio

If a measurement is carried out with an excitation amplitude that is too low, the signal-to-noise ratio will be too high. This first becomes apparent in noise in the phase plot at low frequencies. See Figure 21.

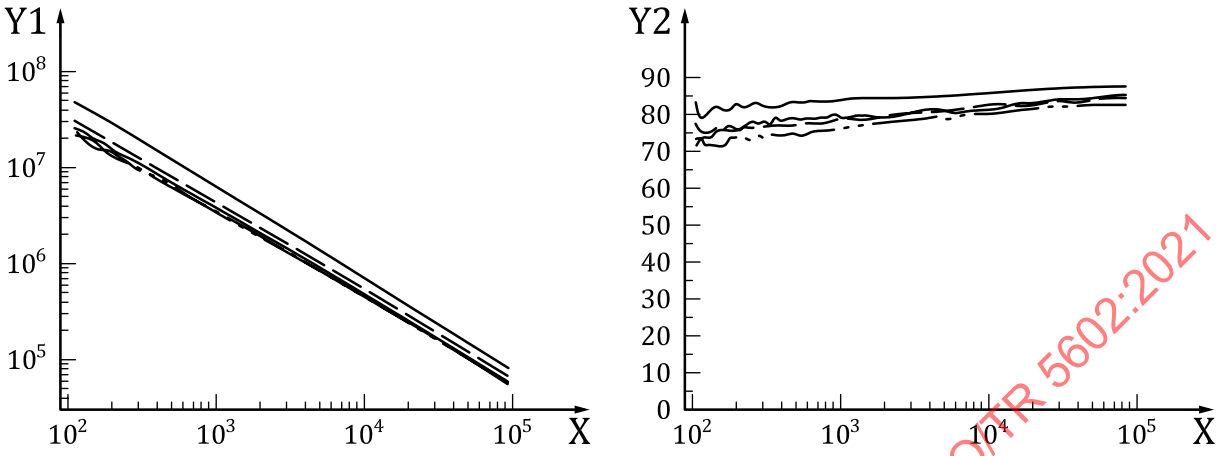

Key

X	frequency f, in Hz
Y1	magnitude of the impedance $\|Z\|$, in $\Omega \cdot cm^2$
Y2	absolute value of the phase angle φ, in degrees
————	t = 0 h
— — —	t = 2 h
- - - - - - - -	t = 24 h
—— · ——	t = 168 h
—— · · ——	t = 504 h

Figure 21 — Influence of too low amplitude leading to a phase plot with a lot of noise

5.9 Influence of peripheral devices

Stirrers, temperature sensors, pumps and measurement devices in the immediate vicinity of the measurement equipment can transmit interference signals to the impedance spectrometer. The antenna effect of a temperature sensor with a connection cable that is too long is shown in Figure 22.

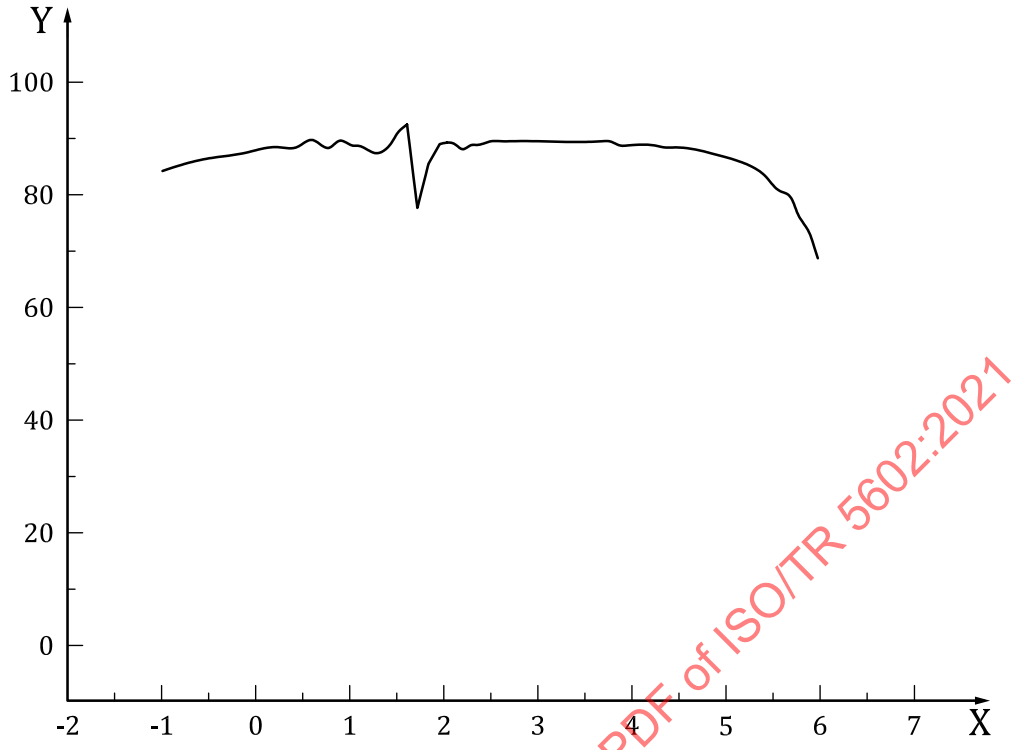

Key

X logarithm of the frequency, *f*, in Hz

Y absolute value of the phase angle, φ, in degrees

Figure 22 — Influence of a temperature sensor with a connection cable that is too long due to antenna effect

An additional influence caused by peripheral devices is shown in Figure 23. Phase plots when a thermostat is switched on and off are shown here.

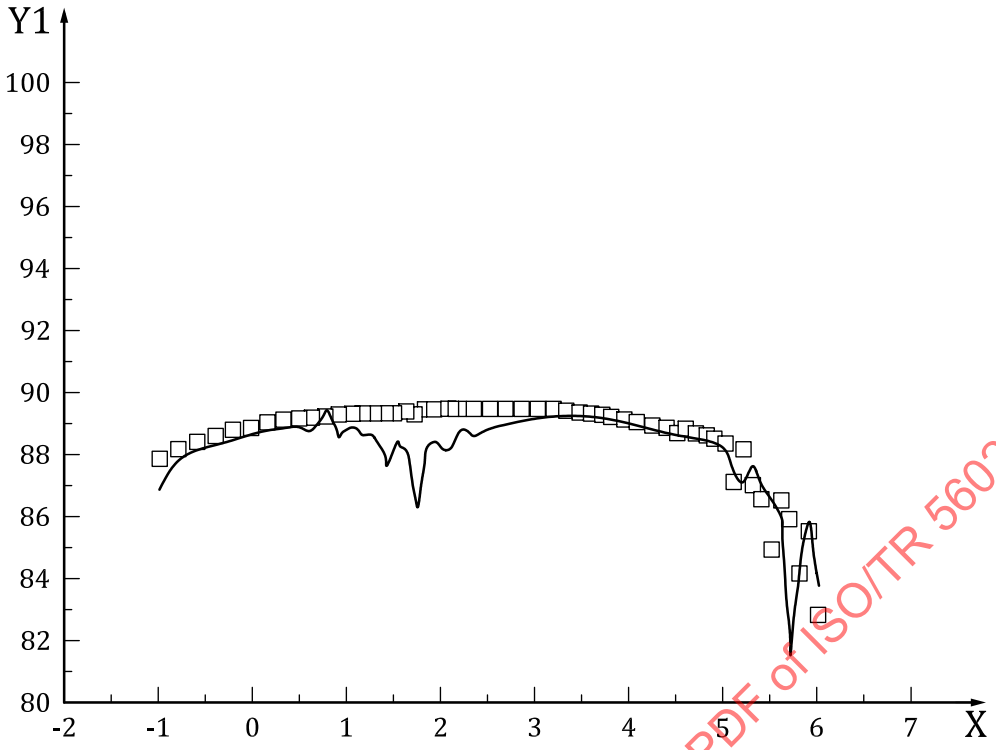

Key

X	logarithm of the frequency, log *f*, in Hz
Y	absolute value of the phase angle, *φ*, in degrees
———	thermostat on
□	thermostat off

Figure 23 — Influence of a thermostat that is switched on and off

6 Parameter selection, measurement range limits

6.1 Open-lead test

Carrying out an open-lead test in accordance with ISO 16773-2:2016, Annex A, provides information about the maximum measurement range of a measurement set-up. Values in the upper limit range are uncertain and associated with significant errors.

6.2 Note on dummy cells – ISO 16773-3

The calibration of the spectrometer is checked with dummy cells at periodic intervals. The resistors and capacitors in the dummy cells correspond to real measurement conditions as closely as possible.

Commercially available dummy cells normally have a component tolerance of between 1 % and 5 %.

6.3 Unsuitable amplitude

Harmonics can occur at amplitudes that are too high. These can easily be identified in a Fourier spectrum (see Figure 24). Nonlinearities can also be detected in a Lissajous figure (see Figure 25). One can clearly recognize the nonlinear behaviour (asymmetry) at an excitation amplitude of 50 mV. A software check for nonlinearities is also carried out, e.g. Kramers-Kronig.

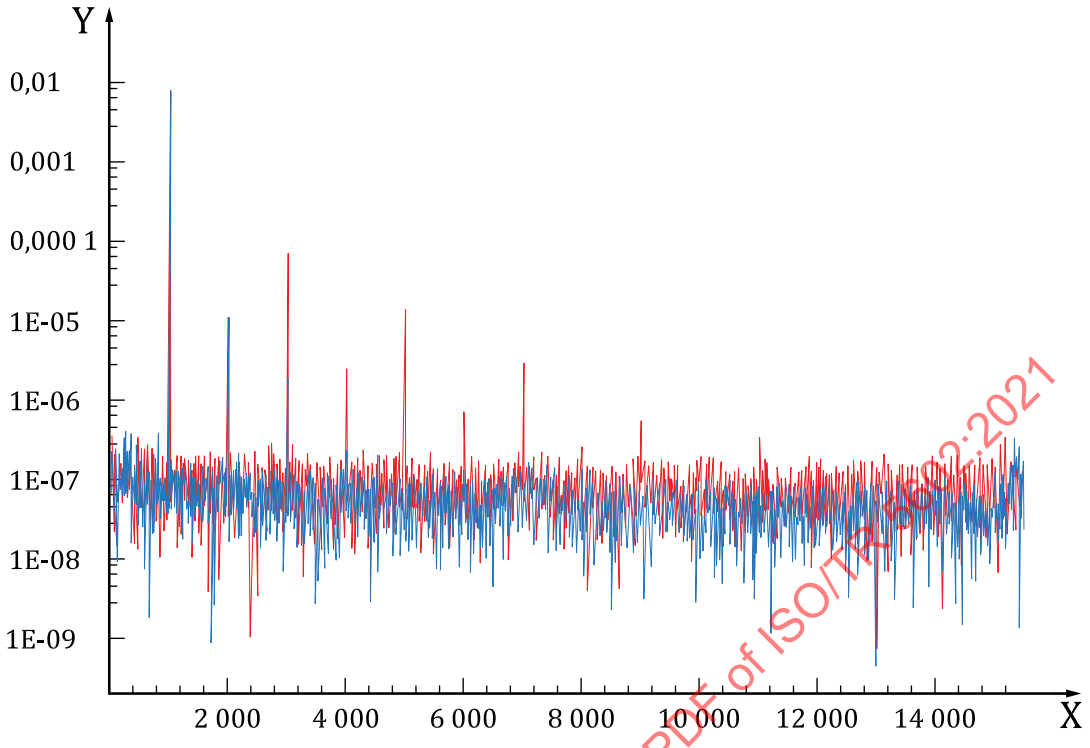

Key

X	frequency, in Hz
Y	current in frequency domain
———	50 mV amplitude
———	10 mV amplitude

Figure 24 — Fourier spectrum with harmonics at 2 kHz, 3 kHz, 4 kHz, etc. (FFT analysis at 1 000 Hz; structural steel in a 1 M NaCl solution at room temperature)

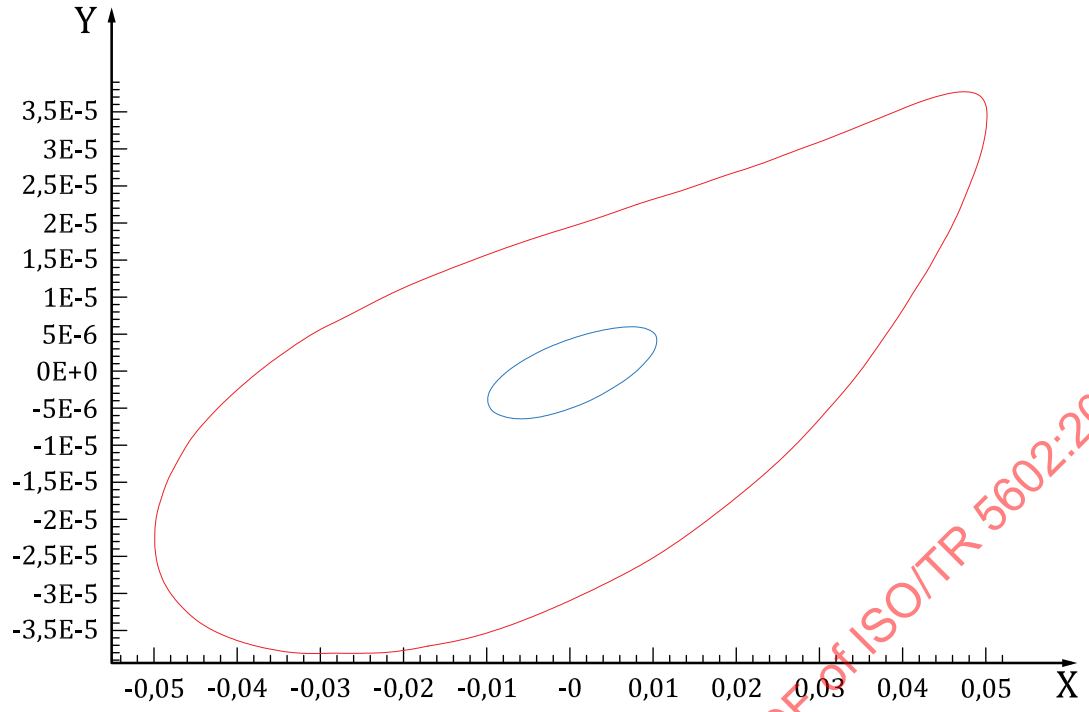

Key

X	potential (AC), in volts
Y	current (AC), in amperes
	50 mV amplitude
	10 mV amplitude

Figure 25 — Lissajous figure for the same measurement at 0,1 Hz

6.4 Insufficient frequency range

If a frequency range that is too small is selected for the evaluation, misleading fit parameters can be obtained. It can be seen in Figure 26 that an apparent resistance of around 800 MΩ (green line) is falsely created when fitting up to 1 Hz as the lowest frequency. However, if the entire frequency measurement range is fitted, the capacitive part is averaged. This can be seen from the significant deviation of the phase angle from the measurement curve (blue line). In contrast, the overall resistance is represented more accurately.

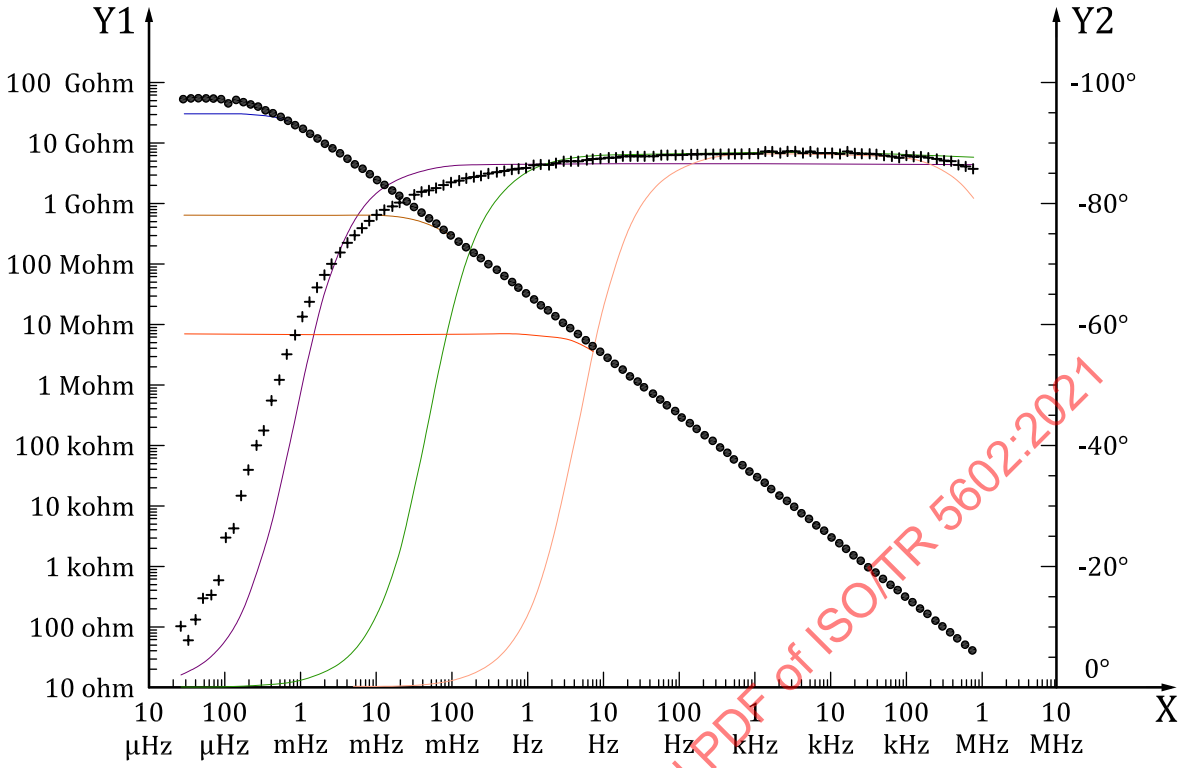

Key

X	frequency, *f*, in Hz
Y1	impedance, *Z*, in Ω
Y2	phase angle, *φ*, in degrees
•	Z curve of a model paint "DTA"
+	(Y2) phase angle of a model paint "DTA"
———	fit of *Z* in the range of 30 µHz until 1 MHz
———	fit of *Z* in the range of 1 Hz until 1 MHz
———	fit of *Z* in the range of 100 Hz until 1 MHz
———	fit of *φ* in the range of 30 µHz until 1 MHz
———	fit of *φ* in the range of 1 Hz until 1 MHz
———	fit of *φ* in the range of 100 Hz until 1 MHz

Figure 26 — Measurement and three fit evaluations for different frequency ranges

6.5 Repetition rate for subsequent measurements

In the case of series of measurements over time, the time intervals between the individual measurements is chosen to be appropriate for the kinetics of the system to be observed.

For the swelling kinetics of coatings, for example, impedance spectra that are as short as possible (e.g. 10 Hz to 100 kHz) are measured in quick succession in the initial period. In this way, it is possible to represent the time change of the system; it is ensured here that the stationarity criteria are fulfilled for the individual measurements. Over the further course of swelling or water absorption, the frequency range and the time intervals between measurements can gradually be increased as long as the stationarity conditions continue to be fulfilled.

7 Non-stationary measurement conditions

7.1 General

If non-stationary conditions are suspected, short measurement times with a limited frequency range are selected to ensure that the individual measurements are pseudo-stationary again.

Figure 27 a) shows the magnitude of the impedance of three consecutive measurements. The measured sample has changed significantly over the course of the first measurement (blue curve). This can be seen from the fall-off in the impedance in the low-frequency range in particular. Even the second measurement (red curve) still shows a slight fall-off. The third curve (green curve) is the first one that appears to be stable.

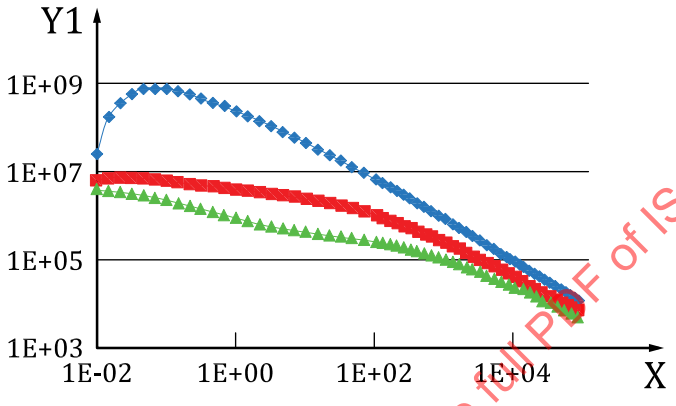

a) Magnitude of the impedance at various points in time of a sample that changes during the measurement

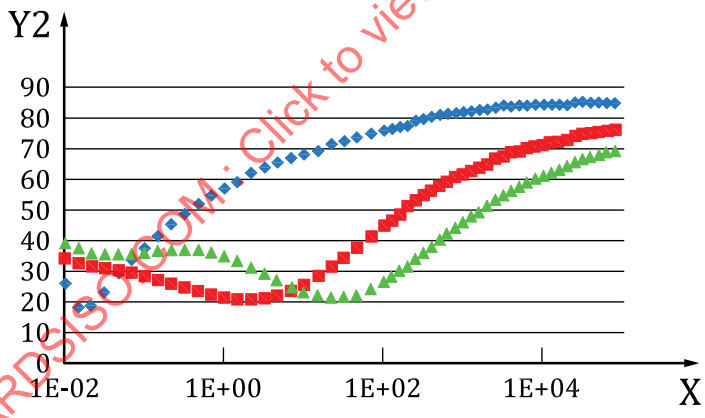

b) Absolute value of the phase angle of the impedance at various points in time of a sample that changes during the measurement

Key

X logarithm of the frequency, log f, in Hz
Y1 logarithm of the impedance, log Z, in $\Omega \cdot cm^2$
Y2 absolute value of the phase angle, $|\varphi|$, in degrees
◆ 0,6 h
■ 0,9 h
▲ 1,2 h

Figure 27 — Bode plot at various points in time of a sample changing during the measurement

7.2 Temperature fluctuations

The resistance of a coating measured with EIS is strongly dependent on the temperature. As a consequence, temperature control is crucial for a proper analysis of coating properties.

It is productive to keep the temperature to ±0,5 °C

Figure 28 shows the strong dependency of the coating resistance on temperature. The logarithm of the resistance increases linearly with the reciprocal of the temperature. The conductivity exhibits Arrhenius behaviour.

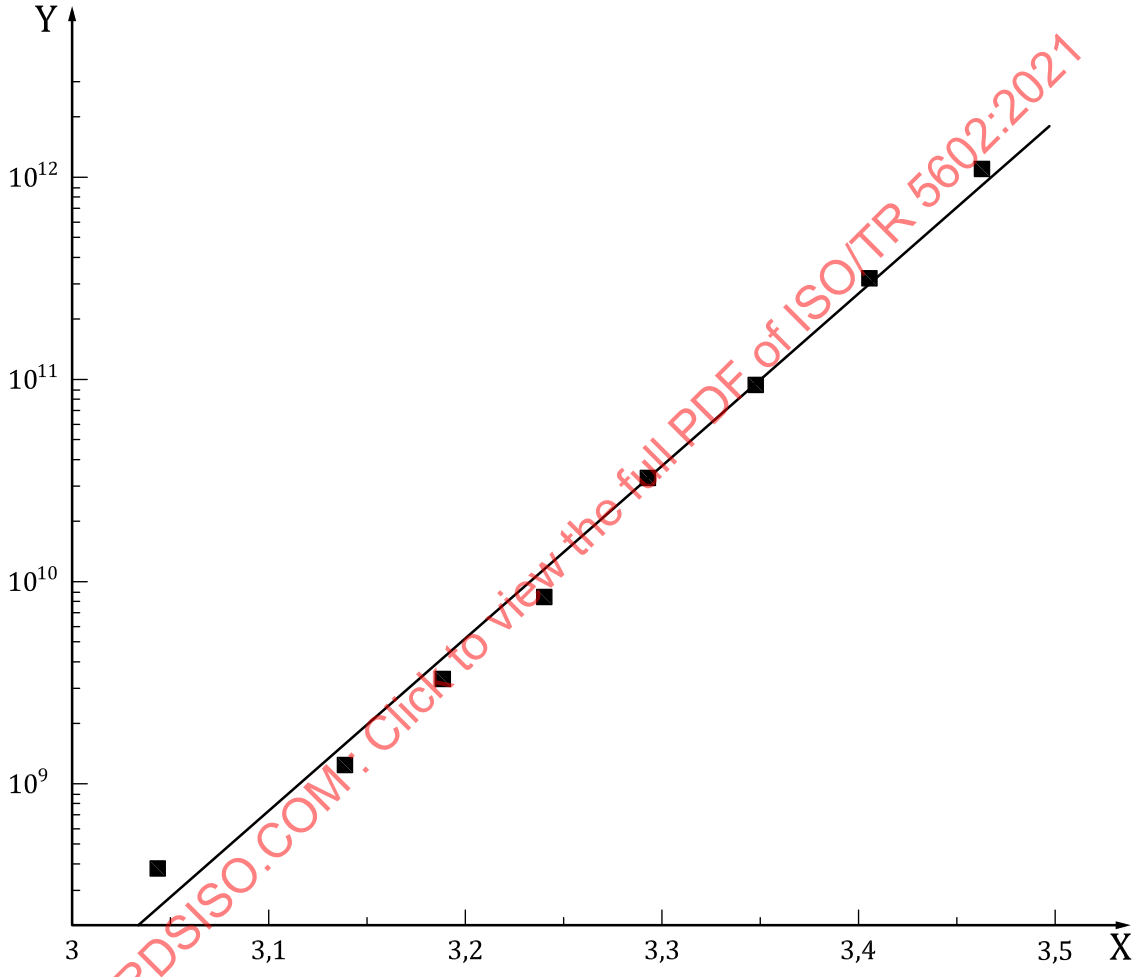

Key

X reciprocal of the temperature, $1000/T$, in K^{-1}

Y resistance, R, in Ω

Figure 28 — Dependency of the coating resistance on temperature

Figure 29 shows the strong influence of a temperature variation on the impedance spectra of coated test panels. In accordance with the temperature profile in Figure 29 a), samples of two coatings with different durabilities were subjected to a temperature change under continuous immersion for five days. Measurements were carried out after two hours at 23 °C, 55 °C and 85 °C. It can be seen in Figure 29 b) that the durable coating withstands this temperature change, as the spectra for each temperature are almost congruent regardless of the immersion period at the relevant temperature. Figure 29 c) shows the analogue impedance spectra of the non-durable coating. Water is increasingly stored in the coating in an irreversible manner due to the influence of continuous immersion and the temperature cycles, which leads to early failure of the coating. The impedance spectra are not grouped in the same manner as in Figure 29 b)[1].

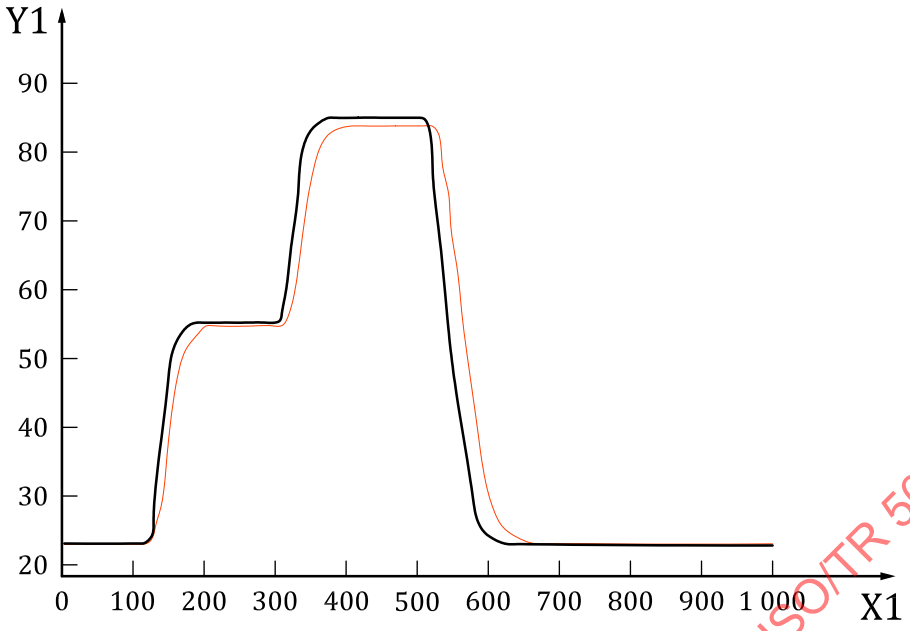

a) Temperature cycle

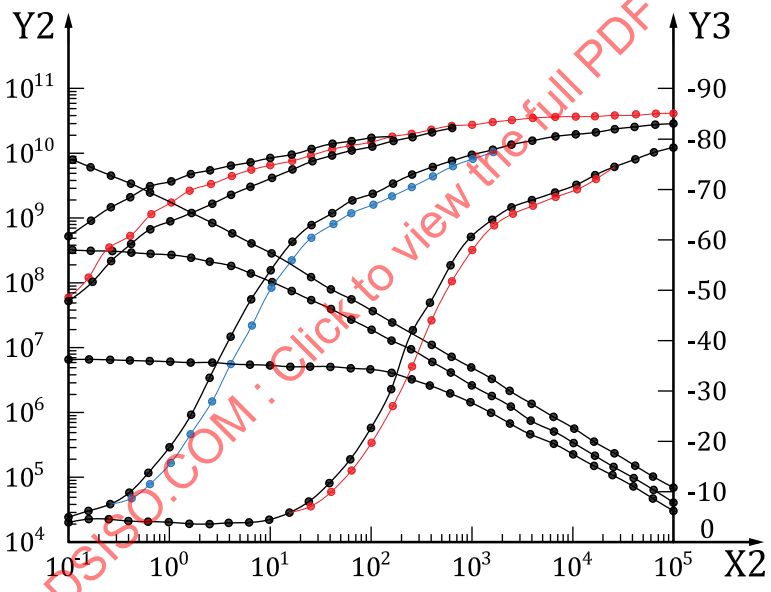

b) Impedance spectra of a durable coating at different temperatures

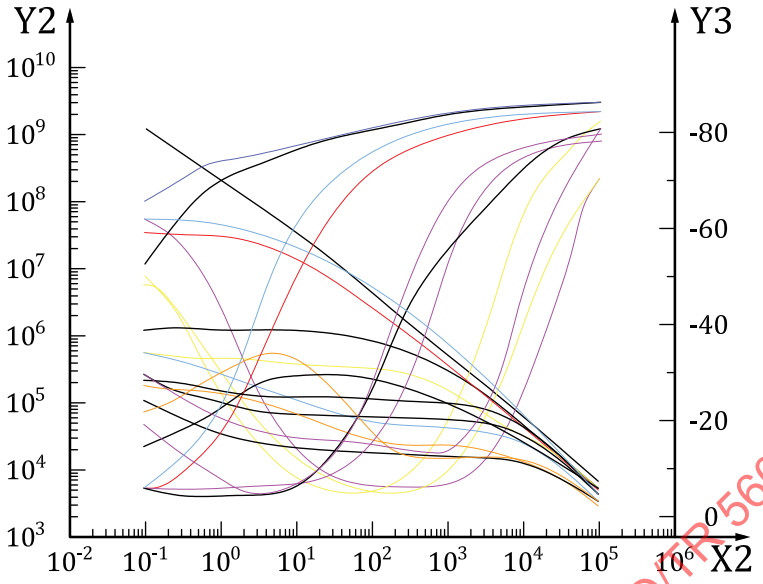

c) Impedance spectra of a non-durable coating at different temperatures

Key

X1	time, *t*, in min
Y1	temperature, *T*, in degrees
———	temperature of the oven
———	temperature of the coating
X2	frequency, *f*, in Hz
Y2	impedance, *Z*, in Ω
Y3	phase angle, *φ*, in degrees

Figure 29 — Temperature influence on impedance spectra of coatings

7.3 Electrolytic conductivity

Extreme salt concentrations, hygroscopic solutions, oxidising and reducing agents, acids or bases are avoided in order to ensure that stationary conditions hold during the measurement. Diluted, inert salt solutions are typically used (e.g. 0,1 to 0,01 molar solutions).

7.4 Swelling

Swelling refers to an increase in the film thickness of a sample due to water absorption. Water absorption and swelling have opposing effects on the coating capacitance. Water absorption increases the capacitance; swelling reduces it. These two processes cannot be separated electrochemically. It is normally assumed that the influence of swelling is low and can therefore be neglected in comparison with water absorption. Some systems can deviate from this assumption, and therefore they are checked.

7.5 Drifting OCP

The open circuit potential (OCP) is not defined in the case of a well-insulating coating and is subject to the influence of electrostatic charge. This leads to false OCP values, which are usually too high. Particular care is exercised if OCPs are measured that are significantly higher or lower than the Nernst potentials.

In the case of water absorption, the coating resistance can change in a relatively short period of time (up to 3 h) by several orders of magnitude (see Figure 30). In this way, the OCP value can return to a reasonable range.

Selecting OCP = 0 V for the first measurement represents a compromise. In the case of inert coatings (without active pigments), the OCP of the substrate can also be used for the first measurement.

Figure 30 a) shows the OCP profile of a coated sample directly after the measuring cell has been filled with electrolyte and after the time periods indicated in the key. An impedance spectrum was measured after each OCP measurement. These are shown in Figures 30 b) and c). It can be seen from Figure 30 a) that unrealistic OCP values are measured (after 0 h and 0,2 h) at the start for the substrate used. Nonetheless, it was possible to measure an impedance spectrum that was meaningful to a large extent, but that exhibited signs of non-stationary behaviour. The coating resistance reduces due to water absorption. The coating is thus more conductive and a realistic OCP value can establish itself as a result. The other impedance spectra were measured at the OCP values present at the times in question.

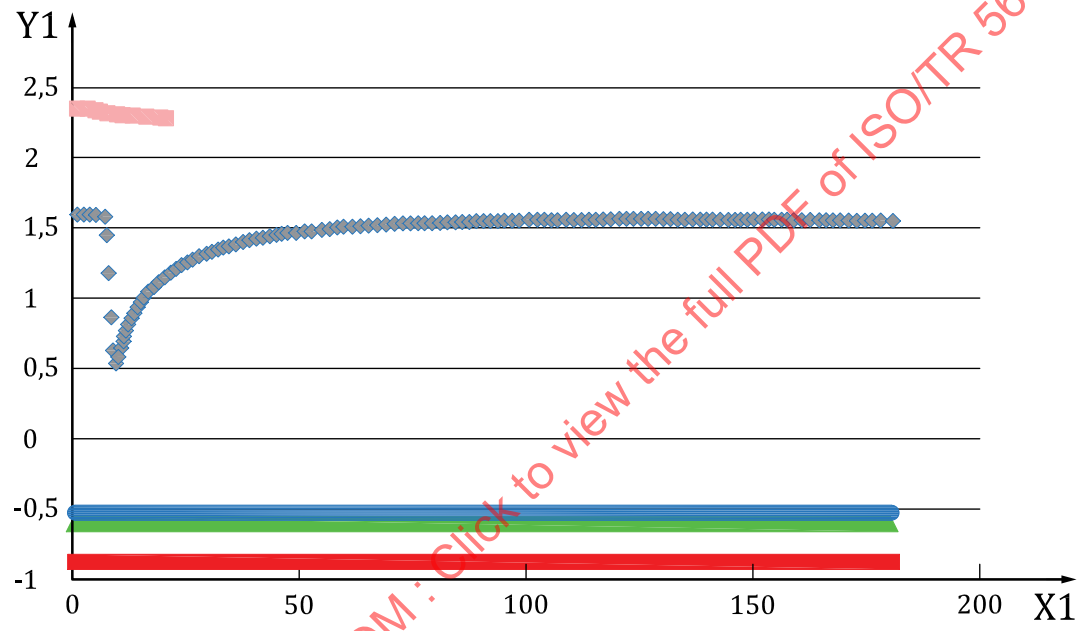

a) OCP time profile after different immersion times

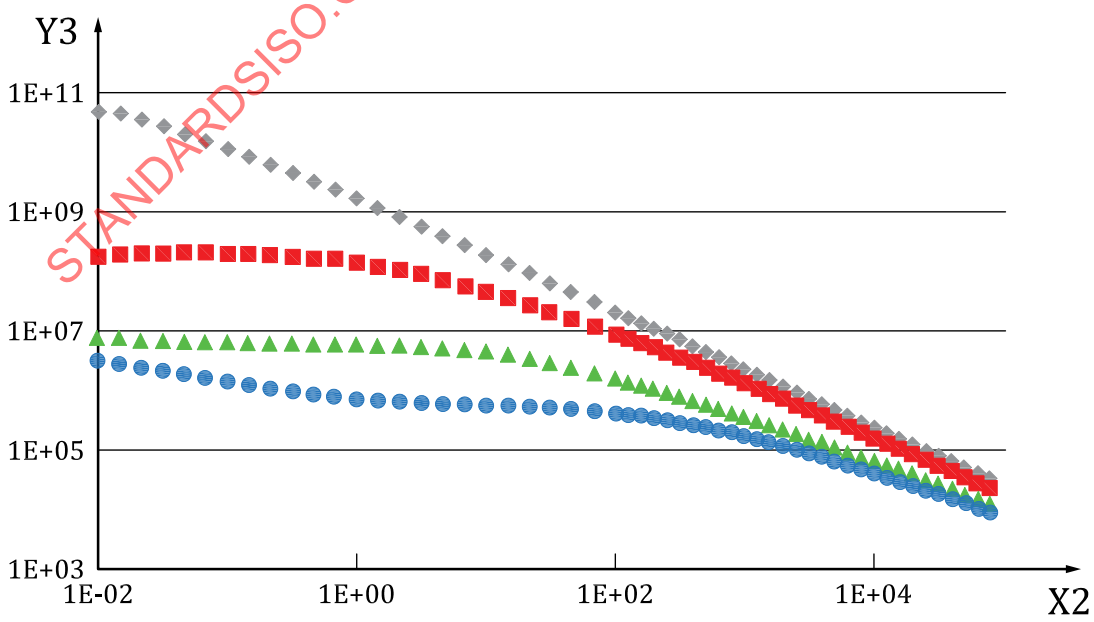

b) Impedance part of the Bode plot with impedance curves at varied immersion times

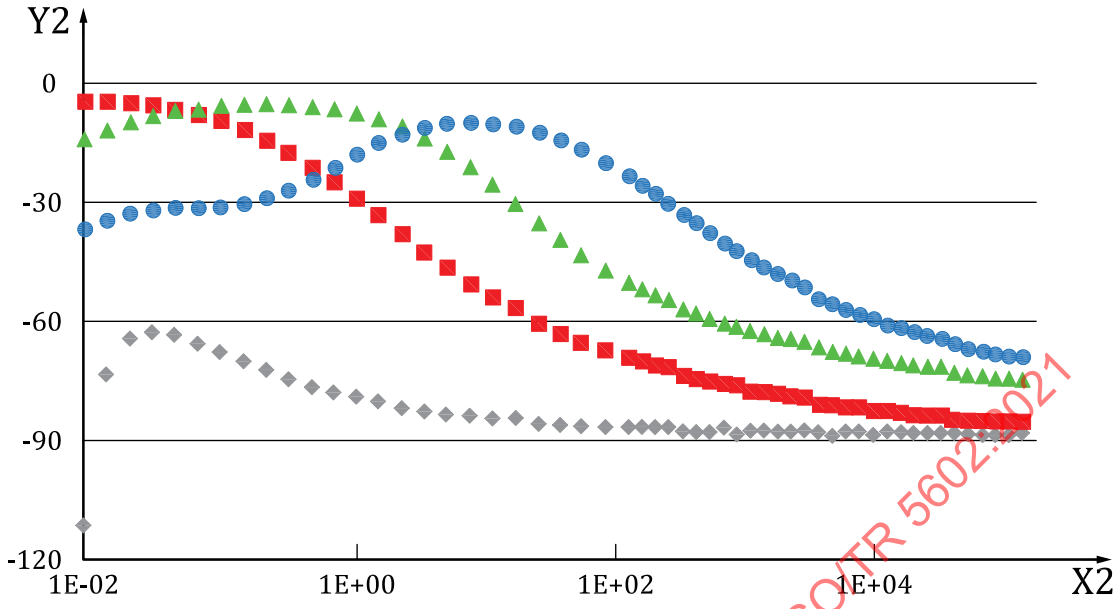

c) Phase part of the Bode plot with phase curves at varied immersion times

Key

X1	time, t, in min
X2	frequency f, in Hz
Y1	open circuit potential, OCP, in V
Y2	phase angle, φ, in degrees
Y3	modulus of the impedance, $\|Z\|$, in Ω
■	0 h
◆	0,2 h
■	4,9 h
▲	45 h
●	114 h

Figure 30 — Series of impedance spectra with an initially unstable OCP

7.6 Corroding working electrode

If the working electrode changes due to the onset of corrosion during the impedance measurement as a result of swelling and the permeation of electrolyte, this becomes evident in the capacitive behaviour. This process is non-stationary and makes it difficult to carry out a meaningful evaluation by fitting equivalent circuit diagrams.

7.7 Reactive counter electrodes

In the case of non-stationary behaviour, reactive counter electrode material can also be the cause of this.

7.8 Gas formation at the counter electrode

Gas is formed as a result of electrolysis in the cell. This gas can shield the surface of the counter electrode.

8 Design and selection of equivalent circuit diagrams

8.1 Constant phase element

Impedance spectra often show non-constant phase profiles for intact coatings in the high-frequency part of the Bode plot; these profiles can be ascribed to the complexity of coatings. The interpretation of a coating as a capacitance would require a constant phase at 90°. The constant phase elements often found in the literature approach these non-constant phase profiles. To this end, the phase angle is adjusted as constant but deviating from 90° in a reference frequency (dotted line in Figure 31). The reference frequency is 10 kHz in Figure 31. The non-constant phase profile is approached somewhat more closely by the parallel combination of resistance and a constant phase element (see the dashed line in Figure 31).

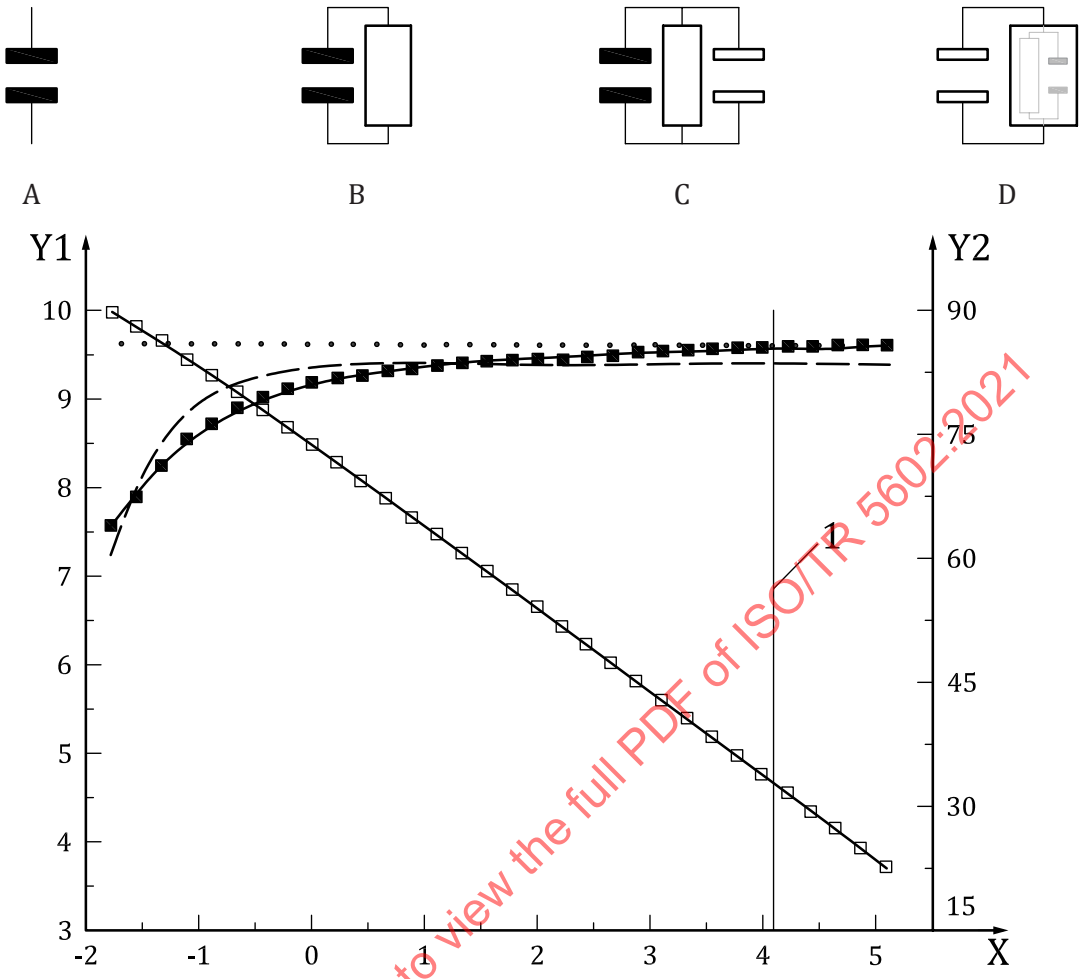

Key

X	logarithm of the frequency, log f, in Hz
Y1	logarithm of the modulus of the impedance, log $\|Z\|$, in Ω cm^2
Y2	absolute value of the phase shift, in degrees
1	normalization frequency of constant phase element
□	measured data $\|Z\|$
■	measured data φ
.	CPE (constant phase element) (A)
— — —	CPE || R (= CPE parallel connected with resistor R) (B)
———	C || CPE || R (= capacitor C parallel to CPE parallel to resistor R) (C) or C || CTRW-2 (= a model consisting of a capacitor C in parallel connection to a two-dimensional Continuous Time Random Walk – process) (D)

Figure 31 — Influence of the constant phase element on the representation of measurement curves

8.2 Multiple possibilities for the selection of equivalent circuits

A measurement can be adapted using multiple equivalent circuits that describe different physical models. Different fitting parameters are then obtained. It cannot be decided on the basis of the quality of fit which of these models is correct. Three models are shown in Figure 32 that show identical curve profiles. A statement about the correct model cannot be made on the basis of the impedance measurement alone.

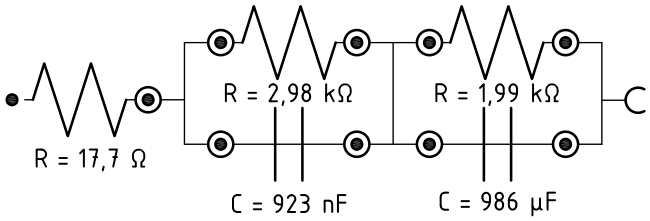

a) Equivalent circuit that is used to describe aluminium surfaces (electrolyte resistance, oxide layer, Helmholtz layer)

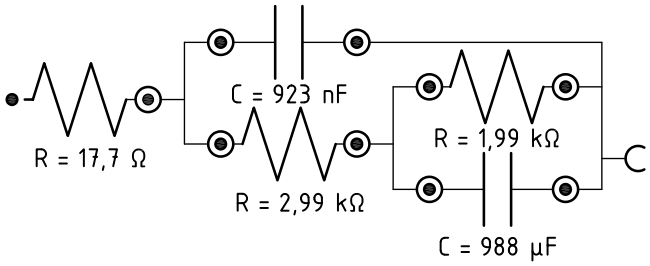

b) Equivalent circuit that is used to describe a porous coating (electrolyte resistance, coating capacitance, pore resistance, double layer)

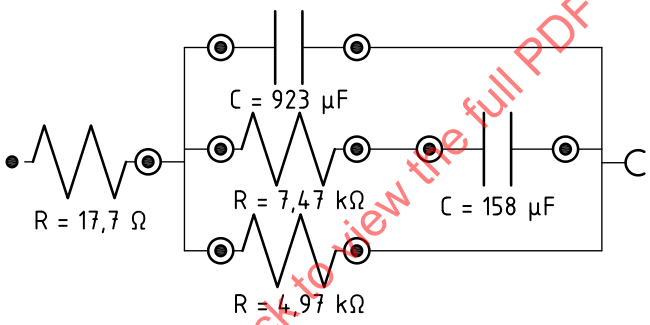

c) Other equivalent circuit that fits the measured data in the same manner as a) and b)

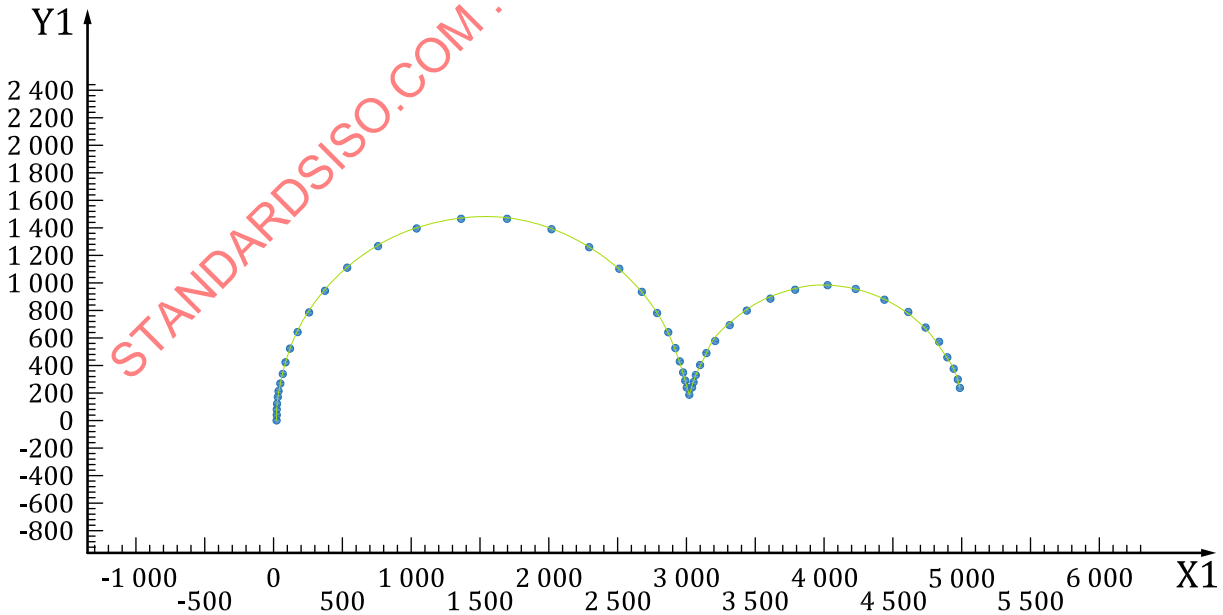

d) Nyquist plot for the equivalent circuits listed

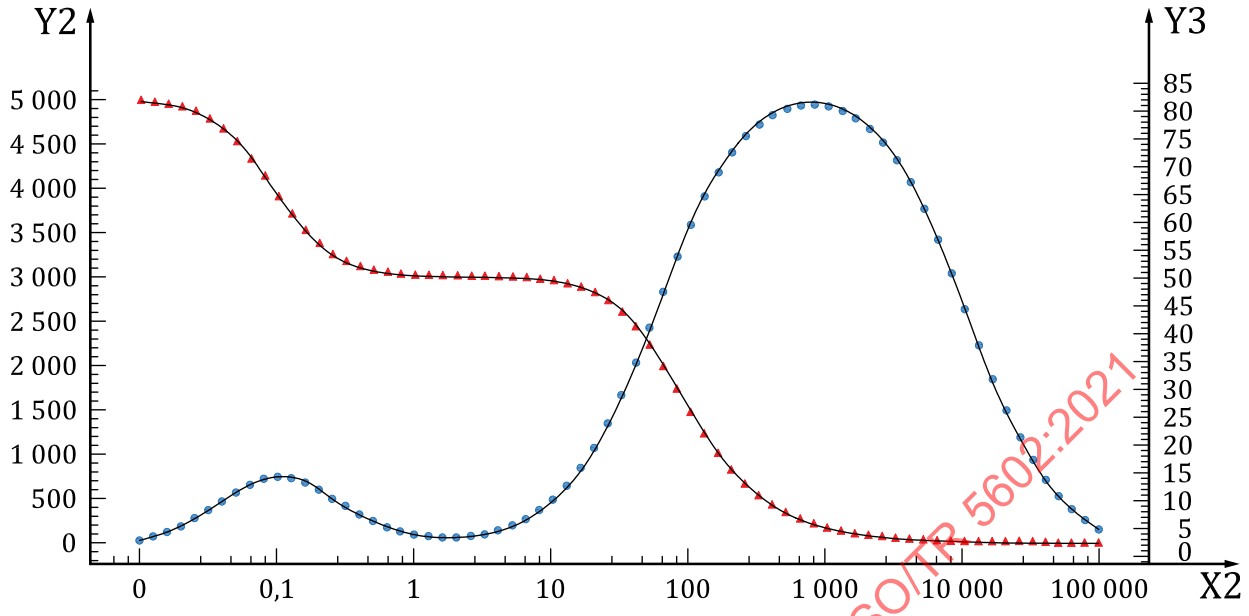

e) Bode plot for the equivalent circuits listed

Key

X1 real part of the impedance, Z', in Ω
X2 frequency, f, in Hz
Y1 negative imaginary part of the impedance, $-Z''$, in Ω
Y2 impedance, Z, in Ω
Y3 absolute value of the phase angle, φ, in degrees

Figure 32 — Representation of the multiple possibilities for the selection of equivalent circuits

8.3 Warburg impedance

An incorrect interpretation due to a lack of basic data can lead to the assumption of a Warburg impedance that is not actually present. The false identification of this behaviour can be caused by measurements in an insufficient large frequency range at low frequencies.

9 Significance of measurement values from equivalent circuits

9.1 Measurement uncertainty

A contour plot illustrates the expected measurement accuracy of an impedance spectrometer. This depends on the specified limit impedances and limit frequencies.

In the contour plot (Figure 33), this corresponds to a measurement uncertainty of 2 % for the impedance $|Z|$ and of 5° for the phase angle for the point (1 000 Hz and 1 MΩ), for example.

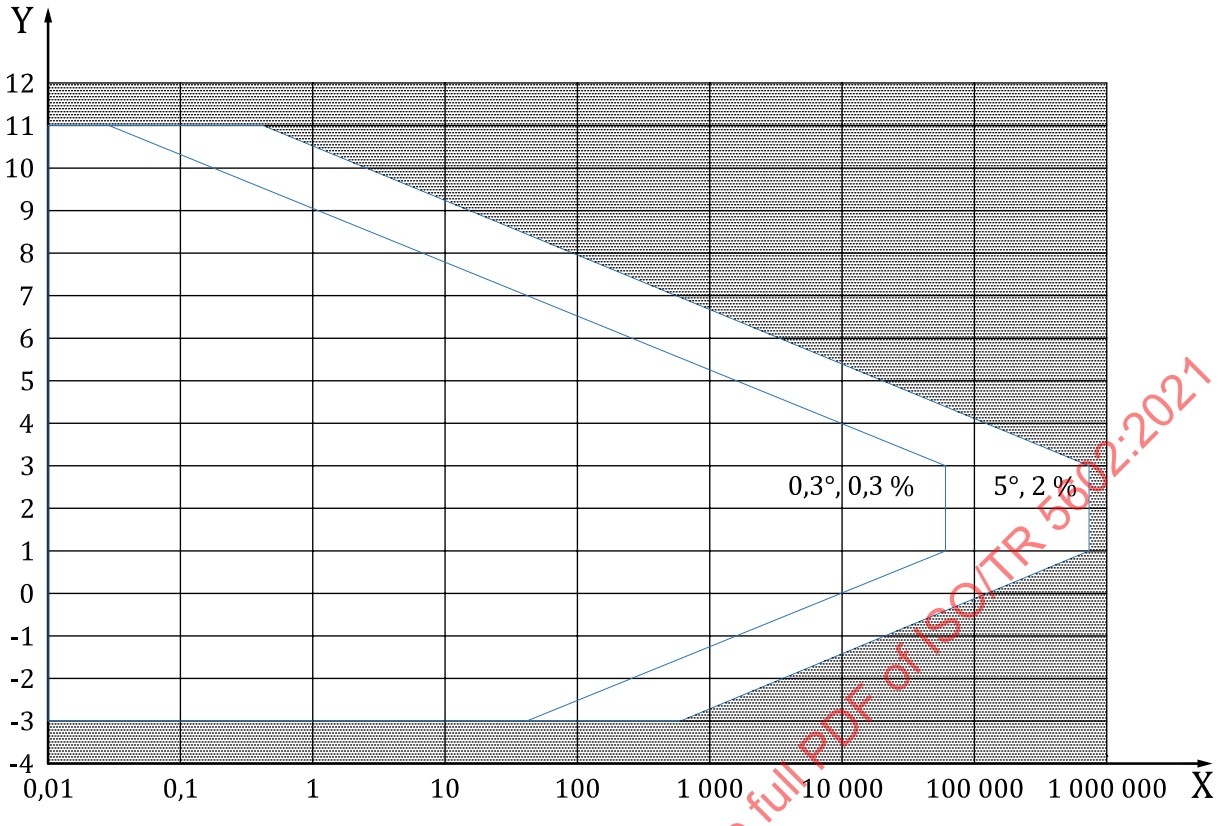

Key

X frequency, f, in Hz

Y logarithm of the modulus of the impedance, log $|Z|$, in Ω

Figure 33 — Example of a contour plot for measurement uncertainty

9.2 Plausibility analysis

The values obtained from fitting are generally subjected to a plausibility analysis. The guideline values given in Table 2 apply here.

Table 2 — Guideline values for typical capacitance ranges

	Typical capacitance ranges
Coating (dependent on material and film thickness)	pF/cm² to nF/cm² – see Annex A
Double-layer capacitance	µF/cm² – see Annex B
Corrosion	mF/cm² – see Annex C

As a complicating factor, the phenomena of corrosion and double-layer capacitance can occur in parallel when the entire surface is considered, i.e. if a pore occupies 0,1 ‰ of the surface and a double-layer capacitance has formed at its base, it is possible that the expected value of 0,1 nF can no longer be separated from the coating capacitance.

10 Interpretation of the measurement values of various coating systems

10.1 Pre-treatment

Pre-treatment of the substrate can have an influence on the impedance spectrum of the system. In the extreme case, the spectrum of the pre-treatment (e.g. anodization) dominates the interpretability of the measurement curves. Two spectra at different points in time for the same coating on non-anodized and anodized plates are shown in Figures 34 a) and b). The change in the coating as a result of ageing can be seen on the non-anodized plate, while this change cannot be detected on the anodizing layer. The reason for this is the barrier behaviour of the anodizing layer.

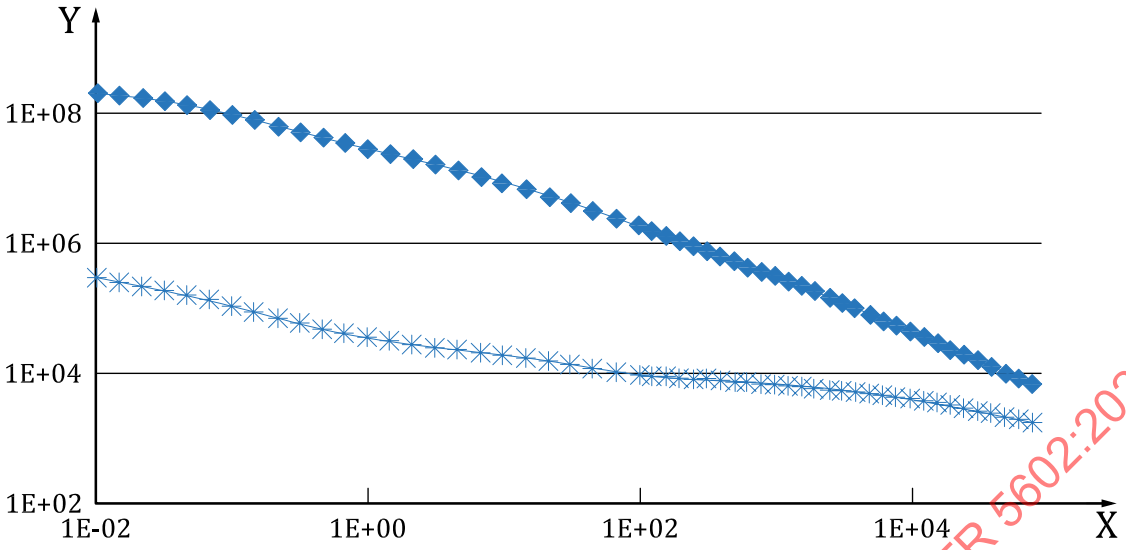

a) Time profile of the spectra for a non-anodized plate

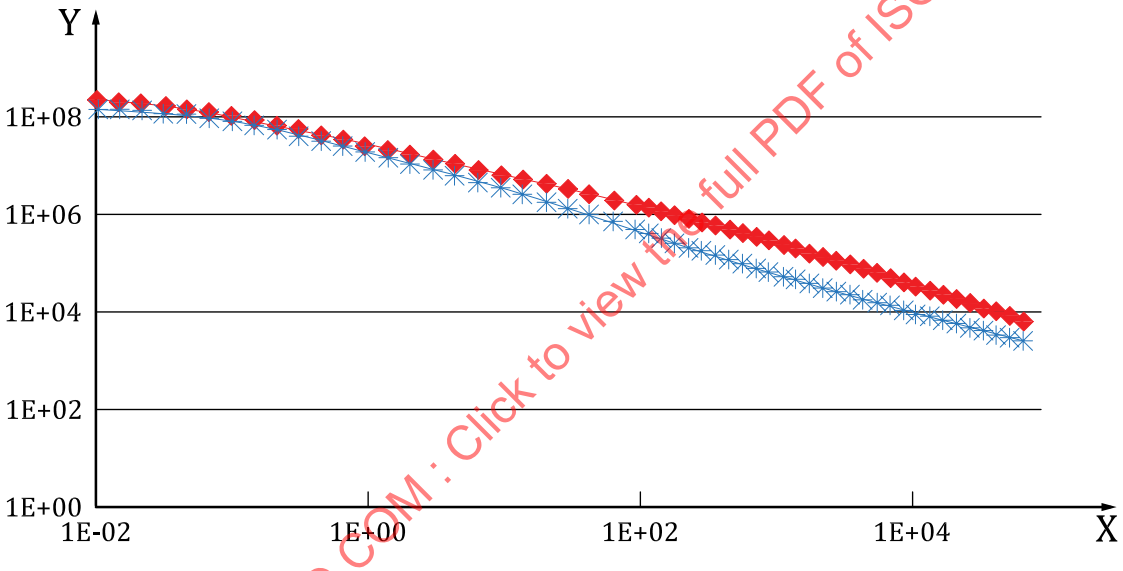

b) Time profile of the spectra for an anodized plate

Key

X frequency, f, in Hz

Y modulus of the impedance, $|Z|$, in Ω

2,7 h

3,3 h

253 h

Figure 34 — Influence of pre-treatment

10.2 Film thickness and measurement surface

The influence of the film thickness is to be taken into account. Examples: 25 µm and 60 µm.

The film thickness of a coating can have an influence on the coating parameters to be determined. Larger deviations can occur for the dielectric constants or the coating capacitance, particularly for small measurement surfaces. This is shown in Figure 35 for the example of a PET film on a metal substrate.

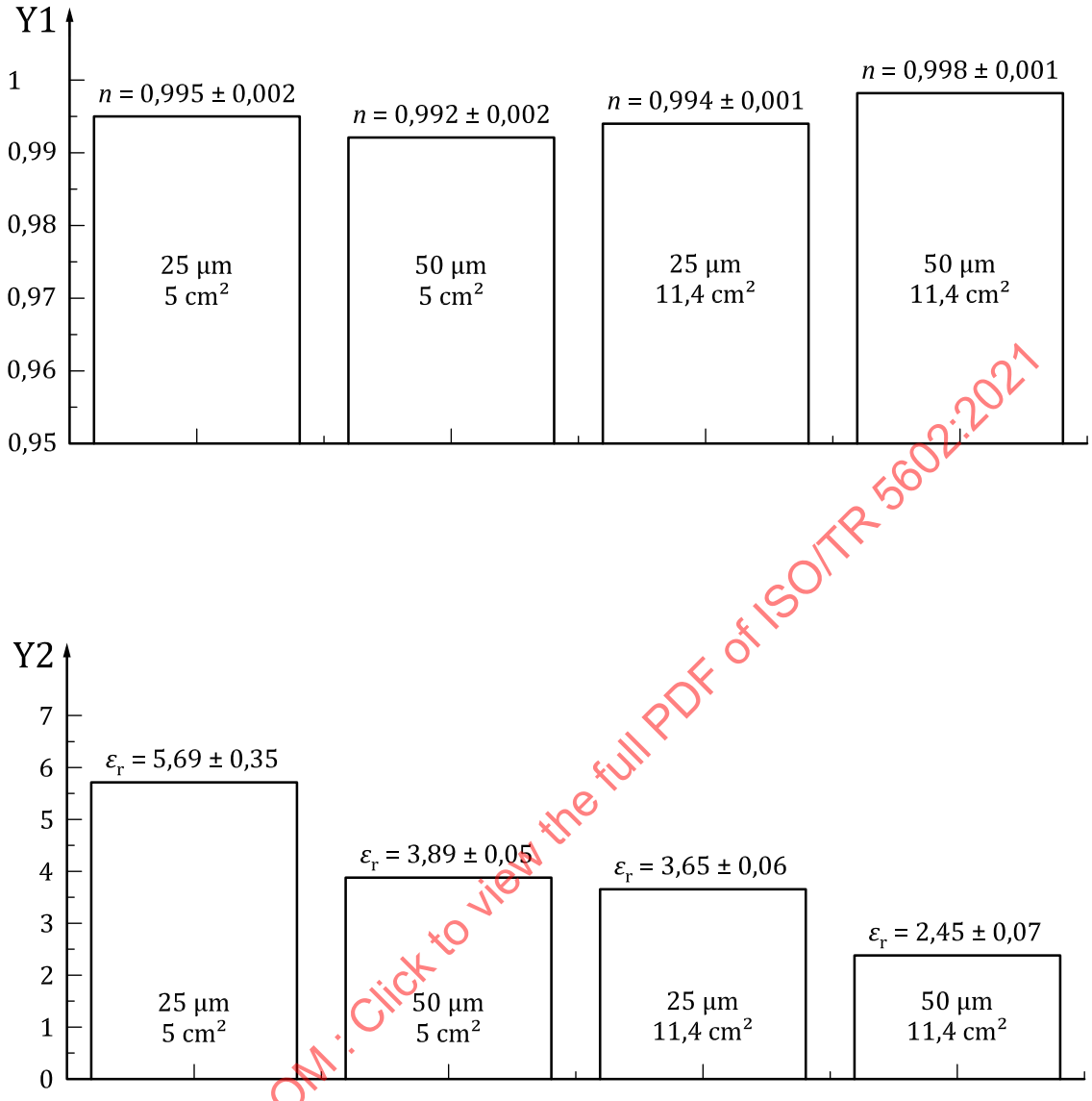

Key

Y1 exponent n of the constant phase element for PET films

Y2 relative dielectric constant, ε_r

Figure 35 — Influence of the film thickness and measurement surface on the exponent of the constant phase element and the dielectric constant

10.3 Number of layers

If a number of coating steps are necessary in order to achieve a target film thickness, each individual application is to correspond to the manufacturer's specifications. Only then is it likely that the film formation for each individual layer will be sufficiently good.

In this example a two-layer coating (2 × 40 µm) (interim drying 60 min at 60 °C, final drying 60 min at 60 °C) was compared to a one-layer coating (1 × 80 µm) (drying 60 min at 60 °C). Coatings were applied on AA 2024 unclad 150 mm × 80 mm × 1 mm abraded with scotch brite. The coating material was a high-solid epoxy-based model coating. A two-electrode setup with a 3 % (mass fraction) NaCl–solution, 16,62 cm² exposed area at (23 ± 2) °C was used.

In Figure 36, a series of spectra is shown over a period of 1 600 h. It can clearly be recognized after 21 h of immersion that the two-layer coating remain at a higher impedance at low frequencies. In the 1st

spectra the ranking between one-coat and two-coat layers is different to the later measurements. Each coating was measured twice.

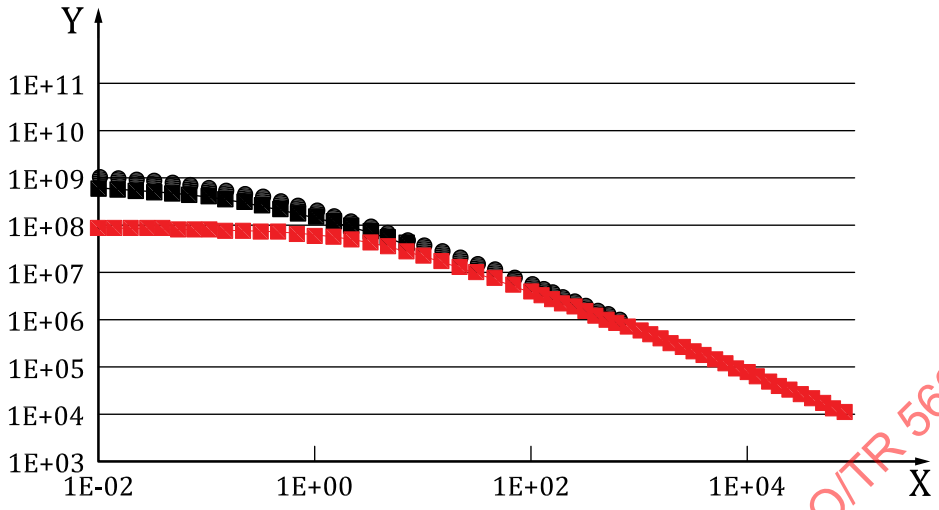

a) 0,5 h

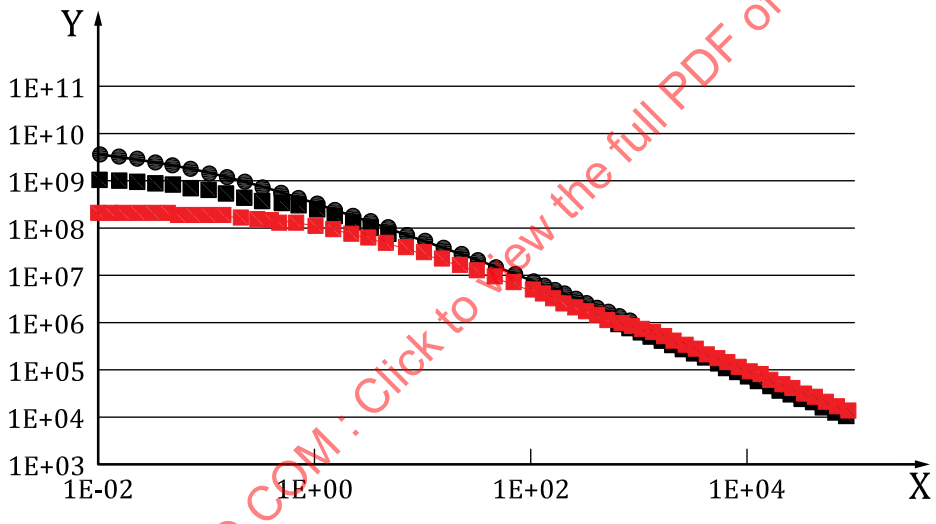

b) 21 h

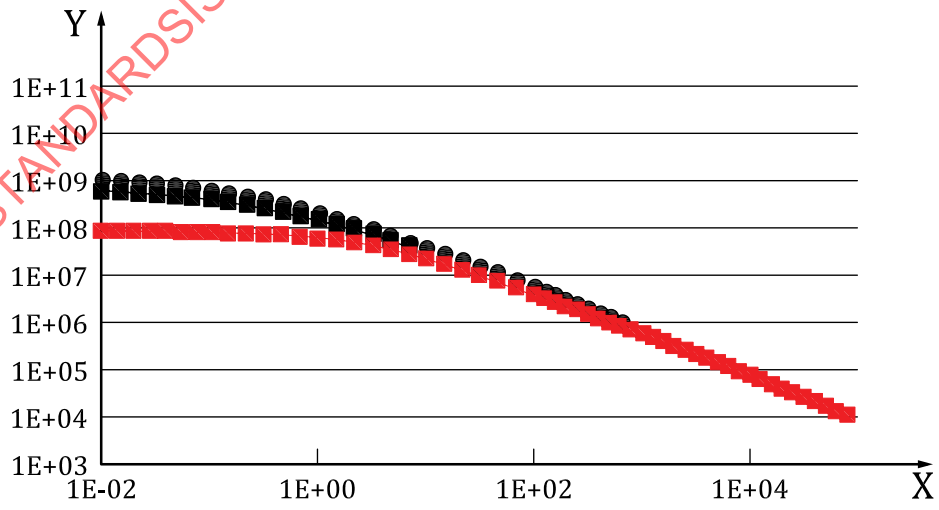

c) 41,5 h